POLARIZATION EFFECT ON RADIATIVE TRANSFER IN PLANETARY COMPOSITE ATMOSPHERES WITH INTERACTING INTERFACE

TSUTOMU TAKASHIMA

Meteorological Research Institute, Tsukuba, Ibaraki, Japan

Abstract. A procedure of computing the radiance and the polarization parameters of radiation diffusely reflected and transmitted by an inhomogeneous, plane-parallel terrestrial atmosphere bounded by a ruffled ocean surface is discussed with the aid of the adding method. If the atmosphere and the ocean are simulated by a number of homogeneous sublayers, the matrices of radiation reflected and transmitted diffusely by the atmosphere-ocean system can be expressed in terms of these matrices of sublayers by using only a couple of iterative equations in which the polarity effect of radiation is included. Furthermore, the upwelling radiance and the polarization degree of radiation at the top of the atmosphere can be calculated by using a single iterative equation without requiring the equation for the diffuse transmission matrix of radiation. The ruffled ocean surface can be treated as an interacting interface, where the transmitted radiation from beneath the ocean surface into the atmosphere is also taken into account into the derivation of equations. Finally, sample computations of the upwelling radiance and the polarization degree of radiation from the top of the atmosphere are carried out at the wavelength of 0.60 micron.

1. Introduction

Remote sensing techniques from the Earth satellites have certain advantages since they make possible frequent observations in the area concerned and with a wide coverage of the Earth. In the visible and adjacent regions of the spectrum, the upwelling radiance at the top of the atmosphere exhibits a very sensitive dependence on the presence of cloud, atmospheric aerosols, ozone and water vapor as well as the optical character of the underlying surface. Therefore this optical dependence could be used as a tool for monitoring such atmospheric constituents as aerosols and ozone from space inversely. In this case the effect of the underlying surface on the upwelling radiation is properly evaluated simultaneously or in advance. More recently, the increased demand for such hydrological information as the aerial coverage of ice and snow as well as the chlorophyll distribution has resulted in the use of remote sensing from the Earth satellites carrying high-resolution radiometers such as MSS of Landsat, CZCS of Nimbus and AVHRR of NOAA satellites. For these investigations the atmospheric effects on the upwelling radiance should be appropriately corrected for satellite borne data. Thus there is a need to find an appropriate algorithm to separate the information interested from the satellite data. This has resulted in a trend to compare satellite borne data with theoretical computations of a more realistic atmosphere-surface model. However, upon computing these upwelling radiation numerically the major difficulties lie in the treatment of the effects of multiple

scattering by various atmospheric constituents. Furthermore the optical characteristics of the underlying surface must be consistently treated.

So far much of the works have been carried out in this field. As for the atmosphere-ocean system is concerned, Raschke (1972) has considered the effect of the ocean wave on radiation in an atmosphere-ocean system by an iterative method. Plass *et al.* (1976) computed the radiance distribution over a ruffled sea by the Monte Carlo Method. Tanaka and Nakajima (1977) examined the effects of the index of refraction of hydrosols and their concentration on the radiation field of the atmosphere-ocean system by the matrix method, which assumed the ocean surface to be smooth. Ueno (1981) obtained the effective surface albedo inversely from space measurements by making use of the quasilinearization, which assumed the ocean surface to be a quasi perfect specular reflector. So far computations of the diffuse radiation field in an atmosphere-ocean system, where the air-water interface is separated by a ruffled ocean surface, has been limited in flux or radiance of the radiation (Nakajima and Tanaka, 1983; Takashima, 1983). This is mainly due to complex treatment of the polarity effect of radiation (Ueno, 1960) upon computing the diffuse radiation field, which is caused by the treatment of the inhomogeneous atmosphere-ocean system.

In this paper, therefore, a treatise on the adding method for the computations of emergent radiation in the atmosphere-ocean system is discussed, in allowing for the polarization effect. In this method the effect of the radiation which is diffusely refracted into the ocean, scattered upwards by such oceanic constituents as water molecules and chlorophyll (hydrosols) and then partly transmitted into the atmosphere is shown to be additive to that of the radiation reflected directly by the ruffled ocean interface. Thus the adding method used for the atmosphere bounded by the ground surface (Takashima, 1984) can effectively be extended to radiative transfer in an atmosphere-ocean system.

2. Basic Equations

Consider an atmosphere which is uniformly illuminated by the parallel radiation of constant net flux $\pi \overline{F}$ (1 × 4 matrix) at the top of the atmosphere in the direction $\Omega_0(-\mu_0, \phi_0)$, where symbols μ_0 and ϕ_0 denote the direction cosine and the azimuth, respectively. In the present work, $\pi \overline{F}$ is normalized to be (1/2, 1/2, 0, 0) in the Chandrasekhar representation of the Stokes vector (Fig. 1). The atmosphere is assumed to be horizontally homogeneous and vertically inhomogeneous, and bounded by a homogeneous ocean surface. The surface is simulated by many facets whose slopes are distributed according to the isotropic Gaussian law with respect to surface wind (Cox and Munk, 1955). The diffusely reflected radiation at the top of the atmosphere-ocean system is expressed by the matrix $\overline{S}^*(\tau_a + \tau_w)$, where symbols τ_a and τ_w represent the optical thickness of the atmosphere and the ocean, respectively. Similarly, the matrix of the diffusely transmitted radiation just above the ocean surface is expressed by $\overline{T}^*(\tau_a)$. The angular dependent reflection and refraction properties of the ruffled ocean surface are calculated based on a Gaussian distribution of wave sloped. When the incident radiation upon the ocean surface
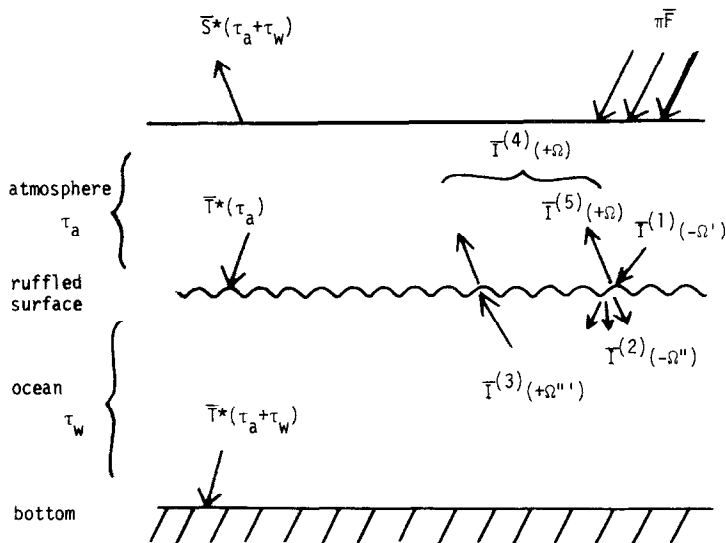
Fig. 1. Diagram showing radiative transfer in the atmosphere-ocean system.

is defined by $\bar{I}^{(1)}(-\Omega')$, where the direction Ω' may be different from that of the solar flux at the top. The corresponding radiation diffusely reflected by the ocean surface and refracted into the ocean are represented by $\bar{I}^{(5)}(+\Omega)$ and $\bar{I}^{(2)}(-\Omega'')$, respectively. The diffusely refracted radiation is reflected diffusely by the oceanic constituents, which is partly transmitted diffusely into the atmosphere and partly reflected diffusely by the air-water interface and then reflected diffusely by the oceanic constituents again. The upward radiation from the ocean after multiple interaction at the air-water interface is represented by $\bar{I}^{(4)}(+\Omega)$. The radiation reflected directly by the ocean surface $\bar{I}^{(5)}(+\Omega)$ is included in the radiation $\bar{I}^{(4)}(+\Omega)$. Similarly the upward radiation just beneath the ocean surface is denoted by $\bar{I}^{(3)}(+\Omega''')$. The sign of solid angle Ω is positive if the direction is upward, whereas it is negative for the downward direction. These diffuse radiations $\bar{I}^{(i)}$ ($i = 1, 2, 3$ and 4) may be expressed by functions of the atmospheric, oceanic and air-water boundary conditions. To obtain the upwelling radiation at the top which is diffusely reflected by the atmosphere-ocean system, or the diffusely transmitted radiation through the atmosphere, a system of these radiations must be solved numerically. Unfortunately this procedure is very complicated, particularly if the polarization effect is included in the radiative transfer. Therefore there is a need to devise a method suitable for numerical computations.

In the adding method, which is suitable for numerical computations, firstly the atmosphere and the ocean are simulated by a number of homogeneous sublayers. Secondly the matrices of radiation reflected or transmitted diffusely by homogeneous sublayers are computed, and then the interaction procedures of radiation reflected and transmitted diffusely by two homogeneous sublayers $x1$ and $x2$ are considered by either starting with

the top of the atmosphere or starting with the bottom of the atmosphere. In the adding method, the underlying surface can be thought of as one of the sublayers (Takashima, 1984). By using the results of radiation reflected and transmitted diffusely by the inhomogeneous sublayer $x1 + x2$, the diffuse radiation by the sublayer $x1 + x2 + x3$, where the sublayer $x3$ is right below or above the sublayer $x2$, can be computed by using the same interaction procedures of radiation as used before. The successive iterations are carried out until the optical thickness $x1 + x2 + x3 + \ldots$ equals the total optical thickness τ. Thus the radiance and the polarization degree of the emergent radiation can be calculated by the matrices of the diffuse radiation of the atmosphere-ocean system.

Let us consider the atmosphere-ocean system. If the sea surface were absolutely calm, a single image of the Sun could be seen reflected on a specular surface. In this case the reflection matrix of a specular surface could be expressed by the following diagonal matrix $\bar{R}_{sp}(n, \chi_t, \chi_i)$ in the Chandrasekhar's representation of the Stokes vector (Chandrasekhar, 1950):

$$
\bar{R}_{sp} = \begin{vmatrix} r_\parallel^2 & & & \\ & r_\perp^2 & & \\ & & -r_\parallel r_\perp & \\ & & & -r_\parallel r_\perp \end{vmatrix} \tag{1}
$$

where elements $r_\parallel$ and $r_\perp$ are given by Born and Wolf (1964) in the forms

$$
r_\parallel = -\frac{n \cos(\chi_i) - \cos(\chi_t)}{n \cos(\chi_i) + \cos(\chi_t)} \tag{2}
$$

and

$$
r_\perp = \frac{\cos(\chi_i) - n \cos(\chi_t)}{\cos(\chi_i) + n \cos(\chi_t)}, \tag{3}
$$

where the ratio of the refractive index of the ocean $n2$ to that of the atmosphere $n1$ is expressed by $n (= n2/n1)$. χ_i and χ_t stand for the incident angle normal to the surface and that of the transmitted radiation, respectively. The incident radiation upon the ocean surface is partly refracted into the ocean, which is partly reflected diffusively by the oceanic constituents and then transmitted into the atmosphere again. However as a first step, the radiation transmitted from the ocean is assumed to be neglected. In this case the effect of the ocean surface upon the reflected radiation can simply be followed by the matrix $\bar{R}_{sp}$ in the form

$$
\bar{R}(A) = 4\pi\mu_0 \bar{R}_{sp}(n, +\Omega, -\Omega_0) \delta(\Omega - \Omega_0), \tag{4}
$$

which is a form suitable for the adding method. The symbol δ represents the Dirac delta function which permits the only monodirectional reflection according to the direction of the incident radiation upon the surface. For a hybrid mode of a diffuse and specular reflector, the reflection matrix can be written in the form

$$\bar{R}(A, +\Omega, -\Omega_0) = \alpha \bar{R}_{\mathrm{L}}(A, \mu, \mu_0) +$$
$$+ (1 - \alpha) \, 4\pi\mu_0 \bar{R}_{sp}(n, +\Omega, -\Omega_0) \, \delta \, (\Omega - \Omega_0), \tag{5}$$

where the symbols $\bar{R}_{\mathrm{L}}$ and $\bar{R}_{sp}$ represent the matrices of the Lambert and specular reflector, respectively. It turns out to be the Lambert reflector at $\alpha = 1$, whereas it is the specular one at $\alpha = 0$ (Takashima *et al.*, 1976).

3. Radiative Transfer of the Interacting Interface

In the visible region of the spectrum, the effect of the radiation transmitted from the ocean into the atmosphere is appreciably noted on the upwelling radiation at the top of the atmosphere. Therefore more precisely, the reflection matrix $\bar{R}(A)$ due to the ocean is composed of a reflection phase matrix of the ocean surface $\bar{R}_G(n, +\Omega, -\Omega')$ where the incident downward radiation is reflected upwards directly by the ocean surface, and a phase matrix of reflection due to scattering in the ocean, $\bar{S}w^u(\tau w, +\Omega, -\Omega')$, where the refracted radiation from the atmosphere into the ocean is reflected diffusely by the water molecules and hydrosols in the ocean and then transmitted upwards to the atmosphere, where for the sake of simplicity, we assume the calm water surface. Consequently $\bar{R}(A)$ is expressed in the form

$$\bar{R}(\tau w, +\Omega, -\Omega') = \bar{S}w^u(\tau w, +\Omega, -\Omega') + \bar{R}_G(n, +\Omega, -\Omega'), \tag{6}$$

where symbol τw denotes the optical thickness of the ocean. In a manner similar to the reflection matrix of radiation $\bar{R}_{sp}$ in Equation (1), the matrix of the refracted radiation $\bar{T}_{sp}$ is given by the following diagonal matrix:

$$\bar{T}_{sp} = |n| \frac{\cos(\chi_t)}{\cos(\chi_i)} \begin{vmatrix} t_{\parallel}^2 & & & \\ & t_{\perp}^2 & & \\ & & -t_{\parallel}t_{\perp} & \\ & & & -t_{\parallel}t_{\perp} \end{vmatrix}, \tag{7}$$

where elements $t_{\parallel}$ and $t_{\perp}$ denote

$$t_{\parallel} = \frac{2\cos(\chi_i)}{n\cos(\chi_i) + \cos(\chi_t)} \tag{8}$$

and

$$t_{\perp} = \frac{2\cos(\chi_i)}{\cos(\chi_i) + n\cos(\chi_t)} . \tag{9}$$

It should be noted that reflectivity ρ and transmissivity t can be related to

$$\rho + t = 1, \tag{10}$$

in agreement with the law of conservation of energy, where ρ and t are expressed by

$$\rho = 1/2 \, (|r_{\parallel}|^2 + |r_{\perp}|^2), \tag{11}$$

$$t = \frac{1}{2} |n| \frac{\cos(\chi_t)}{\cos(\chi_i)} (|t_\parallel|^2 + |t_\perp|^2). \tag{12}$$

It should be noted that reflectivity ρ is transformed into the form:

$$\rho(n, \chi_t, \chi_i) = 1 - 2p \cos(\chi_i) \cos(\chi_t) \times$$

$$\times \left[\frac{1}{(p \cos(\chi_i) + \cos(\chi_t))^2 + (q \cos(\chi_i))^2} + \right.$$

$$\left. + \frac{1}{(p \cos(\chi_t) + \cos(\chi_i))^2 + (q \cos(\chi_t))^2} \right], \tag{13}$$

where p and q are real part and imaginary part of refractive index n, respectively. The refracted radiation into the ocean according to the refraction matrix $\bar{T}_{sp}$, is reflected diffusely by the oceanic constituents, and then partly refracted upwards into the atmosphere. But it is partly reflected by the air-water interface and again reflected by the oceanic constituents. Eventually the transmitted radiation from the ocean would be expressed by infinite modes of multiple reflection and refraction by the air-water interface and reflection by the oceanic constituents.

Cox and Munk made measurements of the sun glitter from aerial photographs (1954). Their measurements covered a wind speed ranging from 0 to $14 \, \mathrm{m}^{-1} \, \mathrm{s}$. They found that there are thousands of 'dancing' highlights in photographs. At each highlight there must be a small water facet which is so inclined as to reflect an incoming ray from the sun towards the observer. To study these surface characteristics, let us consider the average brightness of the sea surface over a sufficiently long time and a sufficiently wide surface area to smooth out fluctuations due to individual glitter sparkles of sunglint. The average is then essentially independent of time but varies smoothly with the azimuth and the elevation of the portion of sea surface under consideration. With this consideration, the ocean surface can be treated as a homogeneous air-water interface. Hence the surface can numerically be simulated by many facets, of which the slope components are according to the Gaussian distribution with respect to surface wind (Cox and Munk, 1955). It is isotropic in the case of the distribution independent of wind direction, but anisotropic in the case of the distribution depending upon wind direction. It should be noted that with the increase of wind speed, the probability of existing white cap, which is formed by thousands of bubbles, increases in the field of view. At present the optical properties of the white cap is not well known. Therefore in the present work, the effect of the white cap on the reflection matrix of radiation is not yet undertaken. In this model surface, parameters χ_i and χ_t are defined by the angles from normal direction to the orientation of facets for the directions of incident and refracted radiation, respectively. According to Snell's law of refraction, these are related to

$$\sin(\chi_i) = |n| \sin(\chi_t), \tag{14}$$

where parameters χ_i and χ_t can be converted to those of the meridian coordinates, where zenith and azimuth are defined by a point on a smooth plane ocean surface, observer and
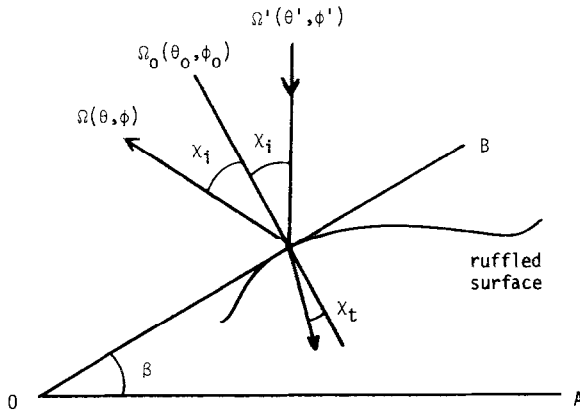
Fig. 2.   Geometry of the facets.

incident solar direction (Takashima and Takayama, 1981). With the aid of this trans-
formation of parameters, the optical characteristics of the ruffled surface can be expressed
by a matrix form suitable for the adding method. The geometry of the facets, show-
ing the incident and reflection directions, are illustrated in Figure 2, where symbols
$\Omega'(\theta', \phi')$, $\Omega(\theta, \phi)$ and $\Omega_0(\theta_0, \phi_0)$ represent the directional parameters, zenith and
azimuth, of incident, emergent directions, and direction normal to the facet, respectively.
The symbols Ω', Ω, and Ω_0 denote solid angles; a line 0A indicates the averaged smooth
plane ocean surface, and a line 0B and an angle β, the direction tangent to a facet and tilt,
respectively. The probability $P(z_x, z_y)$ of the facet within the limits of slope components
$z_x + 1/2 \delta z_x$, $z_y + 1/2 \delta z_y$ is expressed in the case of the isotropic Gaussian distribution
in the form,

$$P(z_x, z_y) = (\pi \sigma^2)^{-1} \exp \left[- (z_x^2 + z_y^2)/\sigma^2 \right], \tag{15}$$

where z_x and z_y represent the slope components in the X- and Y- directions in the sun
vertical and the plane perpendicular to it, respectively. These are measured from the
averaged smooth ocean surface. Cox and Munk (1955) found from airplane photographs
that the mean square slope, regardless of the direction, $\sigma^2 = \langle z_x^2 + z_y^2 \rangle_{AV}$ increases with
the 'masthead' wind speed, w (m^{-1} s), according to

$$\sigma^2 = 0.003 + 0.00512 \times w \pm 0.004. \tag{16}$$

In the presence of a slick this value is reduced by a factor of two or three. The azimuth of
ascent, α, and the tilt, β, are related to the slope components z_x and z_y according to

$$z_x = \sin \alpha \tan \beta, \tag{17}$$

$$z_y = \cos \alpha \tan \beta. \tag{18}$$

The slope components z_x and z_y can be converted to parameters regarding to the incident
$\Omega'(\theta', \phi')$ and reflected $\Omega(\theta, \phi)$ directions with the aid of spherical trigonometry (Taka-
shima and Takayama, 1981) (Appendix A) as

$$z_x = \frac{\sin\theta \ |\sin(\phi - \phi')|}{\cos\theta' + \cos\theta}, \tag{19}$$

$$z_y = \frac{\sin\theta' + \sin\theta \ \cos(\phi - \phi')}{\cos\theta' + \cos\theta}; \tag{20}$$

or there is a useful relation as

$$z_x^2 + z_y^2 = 2a - 1 \quad \text{at} \quad 0 \leq \phi - \phi' \leq 2\pi. \tag{21}$$

Therefore, with the aid of Equations (15), (19), (20), and (21), probability of facets in the isotropic Gaussian distribution can be expressed in the form

$$P(\Omega, -\Omega') = (\pi\sigma^2)^{-1} \exp[(1 - 2a)/\sigma^2], \tag{22}$$

where parameter a is expressed by the zenith angles (θ, θ') and the azimuths (ϕ, ϕ') of the incident and emergent radiation, respectively, in the form

$$a(\theta, \theta', \phi - \phi') = \frac{1 + \cos\theta \cos\theta' + \sin\theta \sin\theta' \cos(\phi - \phi')}{(\cos\theta + \cos\theta')}, \tag{23}$$

where the useful relation between the tilt β and the directions of the incident and emergent radiation is noted as

$$\cos\chi_i \sec\beta = a(\cos\theta' + \cos\theta). \tag{24}$$

Furthermore, the slope parameters $\delta z_x \delta z_y$ can also be converted to the emergent solid angle $d\Omega$ according to

$$\delta z_x \delta z_y = a/(\cos\theta' + \cos\theta)\,d\Omega, \tag{25}$$

where $a > 0$ at $0 < \theta, \theta' < \pi/2$.

Let us derive the reflection matrix of the ocean in a form suitable for the adding method (Figure 1). To derive the optical characteristics of the ocean, the ocean surface and the ocean are separately considered here from the entire atmosphere-ocean system-i.e., without any atmosphere. The diffuse or direct incident radiation upon the ocean surface is defined by $\bar{I}^{(1)}(-\Omega_0)$, where the direction Ω_0 is arbitrary. Hence it may be different from that of the Sun at the top of the atmosphere. Then the upwelling radiation just above the ocean surface $\bar{I}^{(4)}(+\Omega)$ can be expressed mathematically by the reflection matrix of the ocean as

$$\bar{I}^{(4)}(+\Omega) = (1/4\pi\mu)\bar{R}_w(\tau w, +\Omega, -\Omega_0)\bar{I}^{(1)}(-\Omega_0). \tag{26}$$

It should be noted that $\bar{I}^{(4)}(+\Omega)$ is different from the radiation observed just above the ocean surface in the atmosphere-ocean system. In the adding method, the arbitrary incident radiation on the concerned interface is considered to obtain the matrices of the radiation reflected or transmitted diffusely by the sublayer. Hence, the radiation of $\bar{I}^{(4)}(+\Omega)$ in Equation (26) is merely the reflected radiation when the incident radiation upon the surface is specified by $\bar{I}^{(1)}(-\Omega_0)$. The actual radiation observed just above the

surface may be obtained with the aid of the interaction of radiation in the entire atmosphere-ocean system. The matrix $\bar{I}^{(4)}(+\Omega)$ can be written as

$$\bar{I}^{(4)}(+\Omega) = (1/4\pi\mu)\,\bar{S}_w^u\,(\tau_w, +\Omega, -\Omega_0)\,\bar{I}^{(1)}(-\Omega_0) +$$
$$+ (1/4\pi\mu)\,\bar{R}_s(n, +\Omega, -\Omega_0)\,\bar{I}^{(1)}(-\Omega_0). \tag{27}$$

The first term on the right-hand side of Equation (27) is the radiation reflected diffusively in the ocean. This term is additive to the radiation reflected directly by the ocean surface $\bar{R}_s$. Therefore the diffusely reflected or diffusely transmitted radiation in the atmosphere-ocean system can be obtained by placing $\bar{R}_w$ in Equation (26) for the reflection matrix of radiation in the addition method. Thus the ocean surface can be thought of as an interacting interface. Therefore we can avoid the tiresome treatment of the polarity effect caused by the vertically inhomogeneous and horizontally homogeneous atmosphere-ocean system.

When the transmitted radiation just beneath the ocean surface is defined by $\bar{I}^{(2)}(-\Omega')$, the upwelling radiation just beneath the ocean surface $\bar{I}^{(3)}(+\Omega'')$ can be expressed by the reflection matrix of the ocean as

$$\bar{I}^{(3)}(+\Omega'') = (1/4\pi\mu'')\,\bar{S}_w(\tau_w, +\Omega'', -\Omega')\,\bar{I}^{(2)}(-\Omega'), \tag{28}$$

where the reflection matrix of radiation $\bar{S}_w$ is derived by taking into account the scattering of water molecules, hydrosols and chlorophyll apart from the entire atmosphere-ocean system. In the adding method, the diffuse reflection or transmission matrices of radiation in the sublayers are separately computed and then interactions of radiation are undertaken by making use of these matrices. It should be noted that the matrix $\bar{S}_w^u$ is different from that of $\bar{S}_w$, since the radiation refracted into the ocean is not exactly the same as the incident radiation on the ocean surface. Furthermore the radiation from the ocean is refracted by the ocean surface when the radiation is transmitted upwards from the ocean. Let us consider the relation between matrices $\bar{I}^{(1)}$ and $\bar{I}^{(2)}$, and between matrices $\bar{I}^{(4)}$ and $\bar{I}^{(3)}$, respectively, by taking into account the ocean surface characteristics. As for the orientation of a facet, the projected area normal to the incoming rays dS just above the ocean surface is expressed by

$$dS = \cos(\chi_i)\sec\beta\,P(z_x, z_y)\,\delta z_x\delta z_y, \tag{29}$$

where the area projected to the plane parallel to the horizontal smooth ocean surface is put to be unity. With the aid of Equations (22), (24), and (25). Equation (29) can be written as

$$dS = (a^2/\pi\sigma^2)\exp\left[(1-2a)/\sigma^2\right]\,d\Omega. \tag{30}$$

The incident radiation on the facet is, therefore, given by

$$(a^2/\pi\sigma^2)\exp\left[(1-2a)/\sigma^2\right]\,d\Omega\,\bar{I}^{(1)}(-\Omega_0). \tag{31}$$

The reflected radiation by the slope within the limits $z_x \pm 1/2\delta z_x$, $z_y \pm 1/2\delta z_y$, to the direction χ_t upwards is

$$(a^2/\pi\sigma^2) \exp\left[(1-2a)/\sigma^2\right] d\Omega\, \bar{R}_{sp}(\chi_i, \chi_t)\, \bar{I}^{(1)}(-\Omega_0). \tag{32}$$

Therefore, the reflection matrix of the ocean surface $\bar{R}_s$ in Equation (27) can be written as

$$\bar{R}_s(+\Omega', -\Omega_0) = (4a^2\mu'/\sigma^2) \exp\left[(1-2a)/\sigma^2\right] \bar{R}_{sp}(\chi_i, \chi_i). \tag{33}$$

The incident radiation upon the facet $\bar{I}(\Omega')$ is referred to the direction along the meridian coordinates. Hence this vector has to be converted to the parallel and perpendicular to the plane of facet $\bar{I}_i(\omega, \omega')$, which is determined by the directions of the incident radiation, normal to the facet and the reflected radiation as

$$\bar{I}_i(\omega, \omega') = \bar{R}_c(-\alpha)\bar{I}(\Omega'), \tag{34}$$

where $\bar{R}_c(-\alpha)$ is a rotation matrix. Similarly the emergent direction reflected by the facet $\bar{I}(\Omega)$ is expressed in the meridian coordinates in the form

$$\bar{I}(\Omega) = \bar{R}_c(\pi - \beta)\, I_e(\omega, \omega'). \tag{35}$$

The relation between the emergent and the incident radiation is expressed by

$$\bar{I}_e(\omega, \omega') = \bar{R}_G(\omega, \omega')\, \bar{I}_i(\omega, \omega'). \tag{36}$$

With the aid of Equations (34), (35), and (36), we have

$$\bar{I}(\Omega) = \bar{R}_c(\pi - \beta)\, \bar{R}_G(\omega, \omega')\, \bar{R}_c(-\alpha)\, \bar{I}(\Omega'). \tag{37}$$

Therefore, the reflection matrix of the model ocean surface defined by Cox and Munk (1955) is expressed by the form

$$\bar{R}_c(\pi - \beta)\, \bar{R}_G(\omega, \omega')\, \bar{R}_c(-\alpha); \tag{38}$$

or Equation (33) can be written as

$$\bar{R}_s(+\Omega', -\Omega_0) = (4a^2\mu'/\sigma^2) \exp\left[(1-2a)/\sigma^2\right] \times$$
$$\times \bar{R}_c(\pi - \beta)\, \bar{R}_{sp}(\omega, \omega')\, \bar{R}_c(-\alpha). \tag{39}$$

For the Chandrasekhar representation of rotation matrix, it is given by

$$\bar{R}_c(\phi) = \begin{vmatrix} (1+\cos 2\phi)/2 & (1-\cos 2\phi)/2 & \sin 2\phi/2 \\ (1-\cos 2\phi)/2 & (1+\cos 2\phi)/2 & -\sin 2\phi/2 \\ -\sin 2\phi & \sin 2\phi & \cos 2\phi \end{vmatrix} \tag{40}$$

From now on for simplicity rotation matrices are not explicitly shown in derivation of equations.

For a special case of a level surface,

$$\bar{R}_s(+\Omega', -\Omega_0) = 4\pi\mu_0\bar{R}_{sp}(\mu_0); \tag{41}$$

which is equal to the reflection matrix in Equation (4). The refracted radiation by the slope within the limits $z_x \pm 1/2\delta z_x$, $z_y \pm 1/2\delta z_y$, to the direction downwards is similarly written as

$$(a^2/\pi\sigma^2) \exp[(1-2a)/\sigma^2] \, d\Omega \, \bar{T}_{sp}(\chi_t, \chi_i) \bar{I}^{(1)}(-\Omega_0), \tag{42}$$

or by introducing the diffuse refraction matrix of the ocean surface $\bar{R}_T(-\Omega'', -\Omega')$ (Takashima, 1983) according to

$$\bar{R}_T(-\Omega'', -\Omega', n, w) = \frac{4\mu''}{\sigma^2} \exp\left[\frac{1}{\sigma^2}\left(1 - 2b + \frac{1-(1/n)^2}{c^2}\right)\right] \times$$

$$\times \left[\frac{-(1/n)+n}{c} - ncb\right] \left|\frac{b}{c}\right| \times \bar{R}_c(\pi - \beta')\bar{T}_{sp}(-\Omega'', -\Omega', n)\bar{R}_c(-\alpha'), \tag{43}$$

where the direction of the refracted radiation μ'' is related to that of the incident radiation μ' according to Equation (14), and parameters b and c are functions of incident and emergent directions, and of the refractive index of the ocean. Calculations of matrix multiplications in Equations (39) and (43) are shown in Appendix C. The matrix $\bar{I}^{(2)}$ is related to that of $\bar{I}^{(1)}$ as

$$\bar{I}^{(2)}(-\Omega'', -\Omega') = (1/4\pi\mu'')\bar{R}_T(-\Omega'', -\Omega')\bar{I}^{(1)}(-\Omega'). \tag{44}$$

For the radiation reflected diffusely by the water molecules and suspended particles, the upwelling radiation just beneath the ocean surface is expressed by hemispherical integration

$$\bar{I}^{(3)}(+\Omega'') = (1/4\pi\mu'') \int_{2\pi} \bar{S}_w(\tau_w, +\Omega'', -\Omega') \bar{I}^{(2)}(-\Omega') \, d\Omega'; \tag{45}$$

or, by use of the notation introduced by Sekera (1966),

$$\mu'' \bar{I}^{(3)}(+\Omega'') = \{\bar{S}_w(\tau_w, +\Omega'', -\Omega')\mu' \bar{I}^{(2)}(-\Omega')\}. \tag{46}$$

Furthermore Equation (46) can simply be written, without any confusion in the form

$$\mu \bar{I}^{(3)} = \bar{S}_w \, \mu' \, \bar{I}^{(2)}. \tag{47}$$

However, the radiation $\bar{I}^{(3)}$ in Equation (47) is the radiation diffusely reflected only once by the oceanic constituents when the incident radiation refracted into the ocean, $\bar{I}^{(2)}$ is given. The radiation $\bar{I}^{(3)}$ is partly reflected downwards by the atmosphere-ocean boundary and reflected diffusely again upwards by the suspended particles in the ocean. Eventually upward radiation $\bar{I}^{(3)}$ can be expressed by the following infinite series of hemispherical integrations:

$$\mu \bar{I}^{(3)} = \bar{S}_w \, \mu' \, \bar{I}^{(2)} + \bar{S}_w \, \bar{R}'_s \, \bar{S}_w \, \mu' \, \bar{I}^{(2)} + \bar{S}_w \, \bar{R}'_s \, \bar{S}_w \, \bar{R}'_s \, \bar{S}_w \, \mu' \, \bar{I}^{(2)} + \dots, \tag{48}$$

where $\bar{R}'_s$ denotes the same reflection matrix of radiation $\bar{R}_s$ as defined in Equation (27), but for the refractive index which is placed $1/n$ for n. The second term on the righthand side of Equation (48) corresponds to the radiation reflected diffusely downwards by the boundary and reflected again upwards by the suspended particles in the

ocean. The third term corresponds to the radiation where these reflection processes are repeated over again. Equation (48) can be written in a simple form as

$$\mu \bar{I}^{(3)} = \bar{S}_w [\bar{1} - \bar{R}'_s \bar{S}_w]^{-1} \mu' \bar{I}^{(2)}, \tag{49}$$

where the matrix operator $[\bar{1} - \bar{R}'_s \bar{S}_w]^{-1}$ is defined by

$$[\bar{1} - \bar{R}'_s \bar{S}_w]^{-1} = \bar{E} + \bar{R}'_s \bar{S}_w + \bar{R}'_s \bar{S}_w \bar{R}'_s \bar{S}_w + \ldots ; \tag{50}$$

where a proof of Equation (49) is shown at Appendix B. The transmitted radiation from the ocean to the atmosphere $\bar{I}_T^{(4)}(+ \Omega)$ is related to the upwelling radiation from the ocean $\bar{I}^{(3)}(+ \Omega'')$ as

$$\bar{I}_T^{(4)}(+ \Omega) = (1/4\pi\mu) \int_{2\pi} \bar{R}'_T(+ \Omega, + \Omega'') \bar{I}^{(3)}(+ \Omega'') \, d\Omega'', \tag{51}$$

where the reflection matrix of radiation $\bar{R}'_T$ is the same matrix $\bar{R}_T$ as defined in Equation (44), but for the refractie index which is placed $1/n$ for n. Equation (51) can be written by substituting Equations (27), (44) and (49) into Equation (51) as

$$\bar{S}_w^u = \bar{R}'_T \bar{S}_w [\bar{1} - \bar{R}'_s \bar{S}_w]^{-1} \bar{R}_T, \tag{52}$$

when the incident radiation is diffusely reflected or diffusely refracted by the ruffled ocean surface, the diffuse radiation can be obtained by taking a hemispherical integration of the diffuse radiation distributed by the Gaussian law of the facet orientation. Thus the ruffled ocean surface in the diffuse radiation field can be thought of as an additional sublayer where the interaction of radiation is undertaken. This enables us to compute the radiation field reflected or refracted diffusely by the ruffled ocean surface by making use of the adding method.

4. Computational Results and Discussions

To learn about the gross features of the atmosphere-ground system by making use of remote sensing techniques from space, a very extensive knowledge of the optical and physical properties of representative types of naturally occurring aerosols and of natural formations of the lower boundary is required. In this respect, to investigate the atmospheric constituents by remote sensing techniques, the ocean surface is probably better to be chosen as a lower boundary because of its homogeneity and low albedo. With this reason, the radiance and the polarization degree of the upwelling radiation is discussed numerically.

The upwelling radiance at the top of the atmosphere was calculated at wavelength $0.60 \, \mu m$, which corresponds to the center of the wavelength range of channel 1 (0.58–0.68 μm) of the AVHRR radiometer on board the NOAA-7 satellite. This wavelength may also be referred to the visible channel of VISSR on GMS and GOES (0.5–0.75 μm), CZCS on Nimbus 7 (0.54–0.56 μm and 0.66–0.68 μm) and channels of Landsat (0.5–0.6 μm and 0.6–0.7 μm). This wavelength region is slightly off that of maximum

transparency for clear ocean water (about $0.46\,\mu m$) (Plass *et al.*, 1976). The vertical concentration profile of aerosols was given by Selby and McClatchy (1972). Visibility of the atmosphere are 23 and 5 km for clear and hazy conditions, respectively. The aerosols are assumed to be spherical and their size distribution was also given by the authors $(0.02\,\mu m \leqq n(r) \leqq 10.0\,\mu m)$, where the aerosol size distribution function is the same at all altitudes. The size distribution of aerosols is given by the form:

$$n(r) = \begin{cases} C\,10^4 & \text{for} \quad 0.02\,\mu m < r < 0.1\,\mu m \\ C\,r^{-4} & \text{for} \quad 0.1\,\mu m < r < 10\,\mu m \\ 0 & \text{for} \quad r < 0.02\,\mu m \quad \text{and} \quad r > 10.0\,\mu m \end{cases} \tag{53}$$

The constant C is normalized to be for the case of 100 particles with the value of 0.088 24. The scattering phase matrix was computed based on the refractive index of water $(m = 1.332 - i0.0)$ given by Hale and Querry (1973). The optical thicknesses of atmospheric constituents such as aerosols (τ_a), molecules (τ_r) and ozone (τ_o) are given by $\tau_a = 0.161\,87$ and $0.567\,07$ for clear and hazy conditions, respectively, $\tau_r = 0.069\,15$ and $\tau_o = 0.037\,49$. The values of τ_r and τ_o are compiled in the mid-latitude region in summer of the LOWTRAN 5 model atmosphere (Kneizys *et al.*, 1980). Upon computing the emergent radiation, the inhomogeneous atmosphere was simulated by 9 homogeneous sub-layers. The ocean surface was simulated by many facets whose slopes are according to the isotropic Gaussian distribution (Cox and Munk, 1955). The ocean was assumed to be homogeneous and its bottom was assumed to absorb all incident radiation.

A pure water model is assumed for the molecular scattering and absorption. The scattering coefficient of pure water was given by Morel (1974), where the effect of the dissolved salts were ignored. This effect is usually neglected and can be of importance only for the clearest water. The absorption coefficients were obtained from the imaginary part of the refractive index of water given by Hale and Querry (1973). As for hydrosols, a very little knowledge is available. Therefore at the present work, the data compiled by Tanaka and Nakajima (1977) was adopted, where the size distribution of hydrosols is given by the form

$$n(r) = \begin{cases} Cs\,r^{-4}, & \text{for} \quad 0.1\,\mu m < r < 22\,\mu m; \\ 0, & \text{for} \quad r < 0.1\,\mu m \quad \text{or} \quad r > 22\,\mu m; \end{cases} \tag{54}$$

where $n(r)\,dr$ is the number density of hydrosols with radii between r and $r + dr$ and Cs is a constant representing the turbidity condition. For a pure water model, $Cs = 0$, whereas for the clear ocean model $Cs = 300$. Similarly $Cs = 3000$ and $Cs = 30\,000$ for the medium turbid ocean model and the turbid ocean model, respectively. As for the complex index of refraction of hydrosols, two extreme cases, such as $m = 1.16$ and $1.07 - i0.01$, were adopted. The optical thicknesses of hydrosols and water molecules are shown at $\lambda = 0.60\,\mu m$ at Table I.

The incident radiation just beneath the ocean surface is attenuated 99.3% to become only 0.7% of energy when it travels through the ocean water of the optical thickness of 5.

TABLE I

Optical thickness of water molecules and hydrosols

		$m = 1.16$			$m = 1.07{-}i0.01$		
		clear	medium	turbid	clear	medium	turbid
	depth (m)	21.3	17.2	5.9	21.5	19.1	9.0
Hydrosols	ext	0.1322	1.068	3.654	0.069 65	0.6189	2.928
	scat	0.1322	1.068	3.654	0.046 17	0.4103	1.941
Water molecules	ext	4.868	3.932	1.346	4.930	4.381	2.072
	scat	0.023 17	0.018 72	0.006 406	0.023 47	0.020 85	0.009 864
	Total	5.0	5.0	5.0	5.0	5.0	5.0
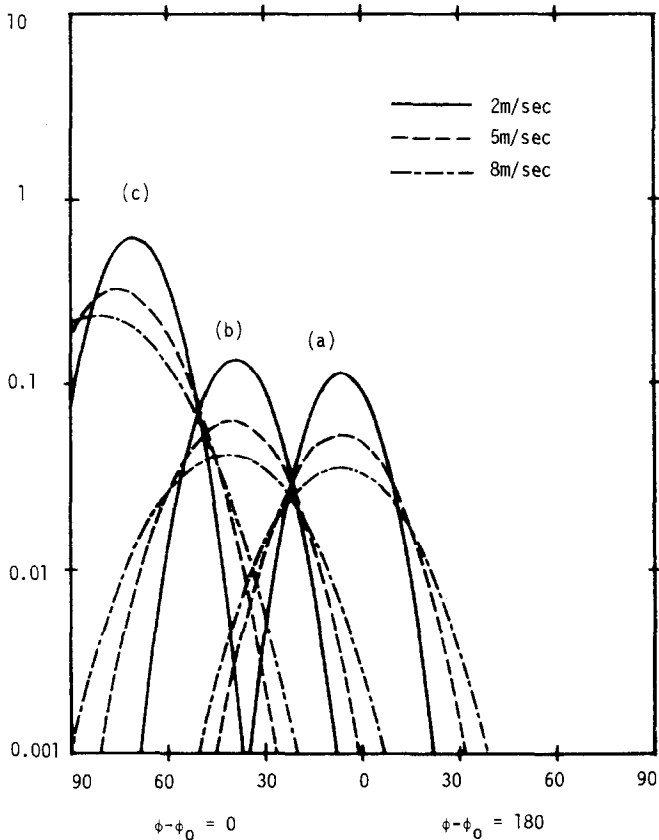
Fig. 3.   Intensity of the upwelling radiation reflected by the surface, where no atmosphere is considered. θ_0 = (a) 6.3°, (b) 38.2° and (c) 66.5°.

Table II

The albedo of the model ocean surface

$w(\mathrm{m\,s^{-1}})$	6.3	22.5	38.2	53.1	66.5	77.6	85.7
2	1.96	1.86	1.83	2.29	3.64	5.41	8.07
5	1.91	1.82	1.81	2.23	3.40	5.28	9.82
8	1.86	1.79	1.79	2.17	3.23	5.23	10.86

Therefore, the contribution of radiation below this depth is neglected. This assumption is equivalent to the condition that the ocean water is bounded by a black body at the depth of this optical thickness. A geometrical depth corresponding to the total optical thickness is also shown in Table I.

The intensities of the radiation reflected by the model ocean surface with no atmosphere are shown in Figure 3 for evaluating the effect of the reflection properties of the ocean surface. Solid, dashed, dashed-dotted lines correspond to the surface wind of $2\,\mathrm{m\,s^{-1}}$, $5\,\mathrm{m\,s^{-1}}$, and $8\,\mathrm{m\,s^{-1}}$, respectively. The flux of the incident radiation is put to be 1. The reflected radiances are given in the principal plane with the solar horizon on the left of Figure 3 ($\phi - \phi_0 = 0°$), the nadir at the center, and the anti-solar horizon on the right ($\phi - \phi_0 = 180°$). Solar zenith angles θ_0 of 6.3°, 38.2°, and 66.5° are shown. The radiation is reflected in accordance with the Gaussian distribution of the facet orientations. Therefore, only around the specular direction, a strong sun glint is noted, which is widely spreaded with the increase of the wind speed. The computational results of the albedo of the surface as a function of the solar zenith angles are shown in Table II (Takashima and Takayama, 1981). Here the albedo of the surface is defined by the ratio of the flux of the radiation reflected upwards by the surface to the incident flux upon the surface at the given zenith angle θ_0. In Table II, 2%, 2% or 3.6% of the incident radiation is reflected by the ocean surface at $\theta_0 = 6.3°$, 38.2° or 66.5°, respectively, with the surface wind of $2\,\mathrm{m\,s^{-1}}$. In other words, 98%, 98% or 96.4% of the incident radiation is penetrated into the ocean for the corresponding incident direction. The intensity is relatively high at the higher zenith angles of observation due to the high reflectivity of the ocean surface.

Figure 4 shows intensity of the upwelling radiation from the atmosphere bounded by the model ocean surface with the wind speed of $2\,\mathrm{m\,s^{-1}}$ (AS), where the clear (c) and hazy (h) atmospheric conditions are considered. Intensity of the hazy condition is larger than that of the clear condition due to scattered radiation in the atmosphere. For evaluating the surface reflection property, the upwelling radiance of the radiation from the atmosphere without any lower boundary is also shown in Figure 4 (A). The strong sun glint is noted around the specular direction for $\theta_0 = 6.3°$ and 38.2°. It is stronger for a clear condition than can be seen for a hazy condition, due to the extinction and scattering in the atmosphere when the incident solar radiation penetrates into the atmosphere, reflected by the surface and travels through the atmosphere. However off the sun glint, the intensity of the upwelling radiation approaches to that from the atmosphere without
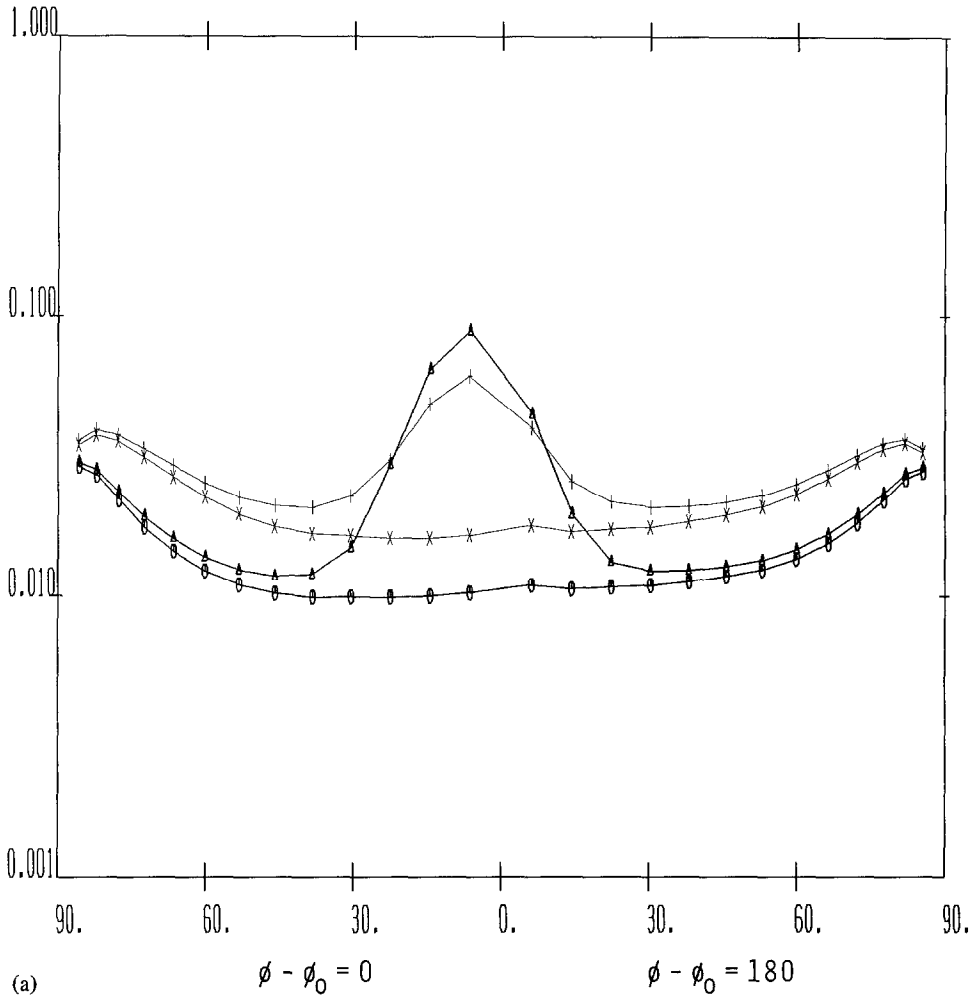
Fig. 4.   Intensity of the upwelling radiation from the atmosphere bounded by the model ocean surface. $w = 2\,\mathrm{m\,s^{-1}}$. The symbols $\circ$, $\triangle$, $\times$, and $+$ denote A-c, AS-c, A-h and AS-h, respectively. $\theta_0 =$ (a) $6.3°$, (b) $38.2°$ and (c) $66.5°$.

surface reflection. Especially when the nadir angle of the incident solar radiation is large, no appreciable difference is seen on the anti-solar side ($\phi - \phi_0 = 180°$) (Figure 4b and c). Table III shows the albedo of the atmosphere with and without the lower boundary as a function of the incident solar direction. Here the albedo is defined by the ratio of the flux of the upwelling radiation from the atmosphere to the incident solar flux at the top. The albedo increases monotonically with the increase of the nadir angle of the incident solar radiation. It is higher in the hazy condition than in the clear condition due to the scattering in the atmosphere. No appreciable difference of the albedo value is seen with respect to the surface wind change. Figure 5 shows the same results as Figure 4, but for

(b) $\phi - \phi_0 = 0$ $\phi - \phi_0 = 180$
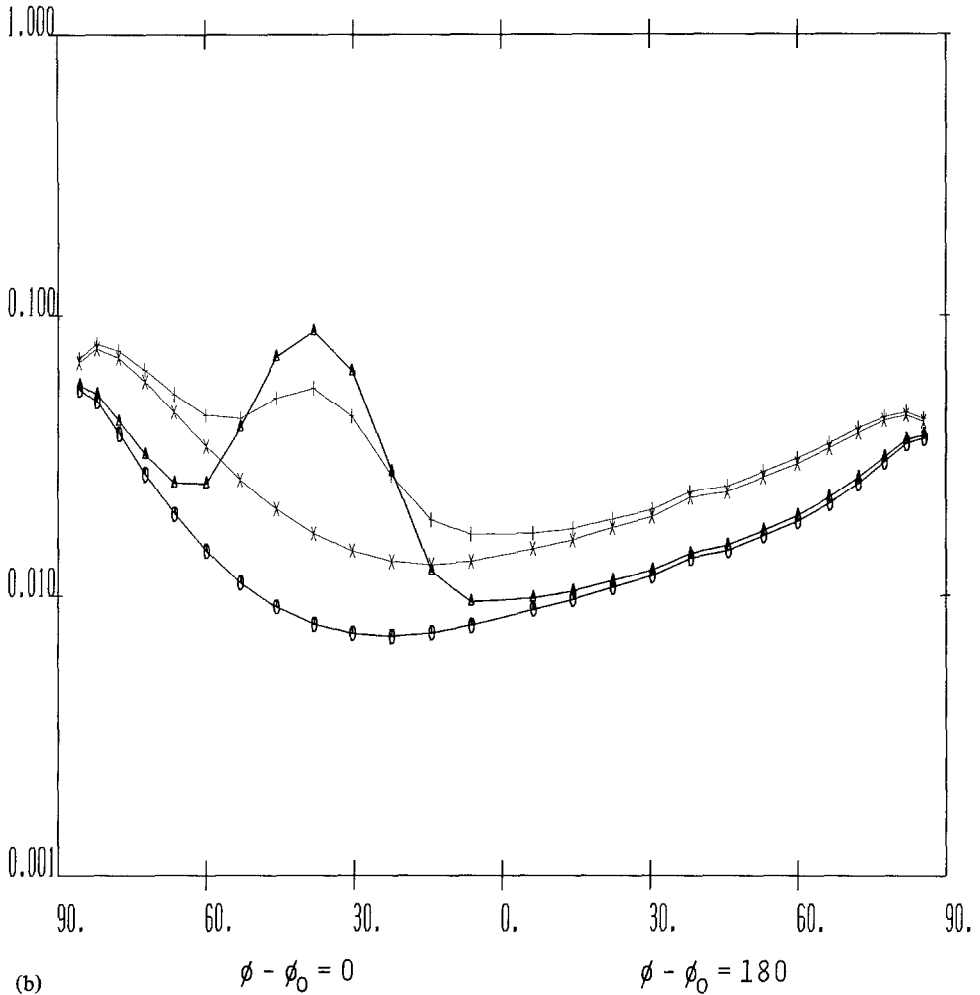
Fig. 4. *Continued.*

the degree of polarization. At the incident solar direction of $6.3°$ (Figure 5a), the polarization degree does not show any appreciable difference between the case of the atmosphere bounded by the ocean surface and that of the atmosphere only. It shows a slight effect on the atmospheric condition in the nadir (zenith) angles over $40°$. In this angles, the polarization degree is higher in the clear condition than in the hazy condition. In the case of the incident nadir angle of $38.2°$ (Figure 5b), the polarization degree is high in the sun glint. The peak value is 85% and 65% in the clear and hazy conditions, respectively with the wind speed of $2\,\mathrm{m\,s^{-1}}$. This is higher than that of the atmosphere only. As for the atmosphere only, the corresponding peak value is 70% and 44% in the clear and hazy conditions, respectively. This is mainly due to the contribution of the polarized radiation resulted by the reflection process. Therefore it depends upon the ocean surface wind.

(c) $\phi - \phi_0 = 0$ $\phi - \phi_0 = 180$
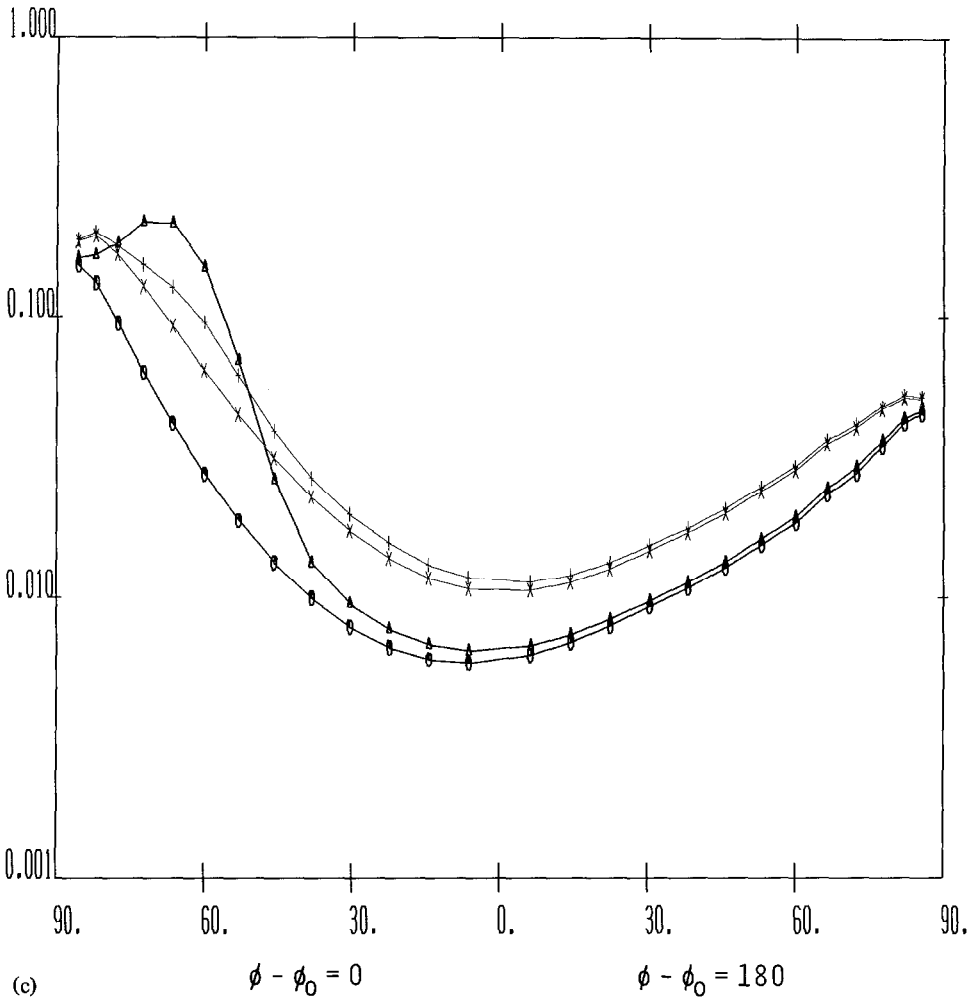
Fig. 4.   *Continued.*

TABLE III

The albedo (%) of the atmosphere with and without the ocean surface

		$w(\text{m s}^{-1})$	6.3	22.5	38.2	53.1	66.5	77.6	85.7
A-only	c		3.96	4.31	5.21	7.16	11.32	19.63	28.12
	h		6.57	7.30	9.20	13.17	20.60	30.93	33.27
		2	5.68	5.94	6.78	8.93	13.47	21.62	29.05
A-S	c	5	5.64	5.90	6.76	8.89	13.39	21.68	29.12
		8	5.59	5.87	6.74	8.85	13.34	21.71	29.16
		2	8.20	8.85	10.69	14.71	22.14	32.04	33.81
A-S	h	5	8.16	8.82	10.66	14.68	22.11	32.05	33.81
		8	8.12	8.79	10.64	14.65	22.09	32.05	33.81

$\phi - \phi_0 = 0$ $\phi - \phi_0 = 180$

(a)
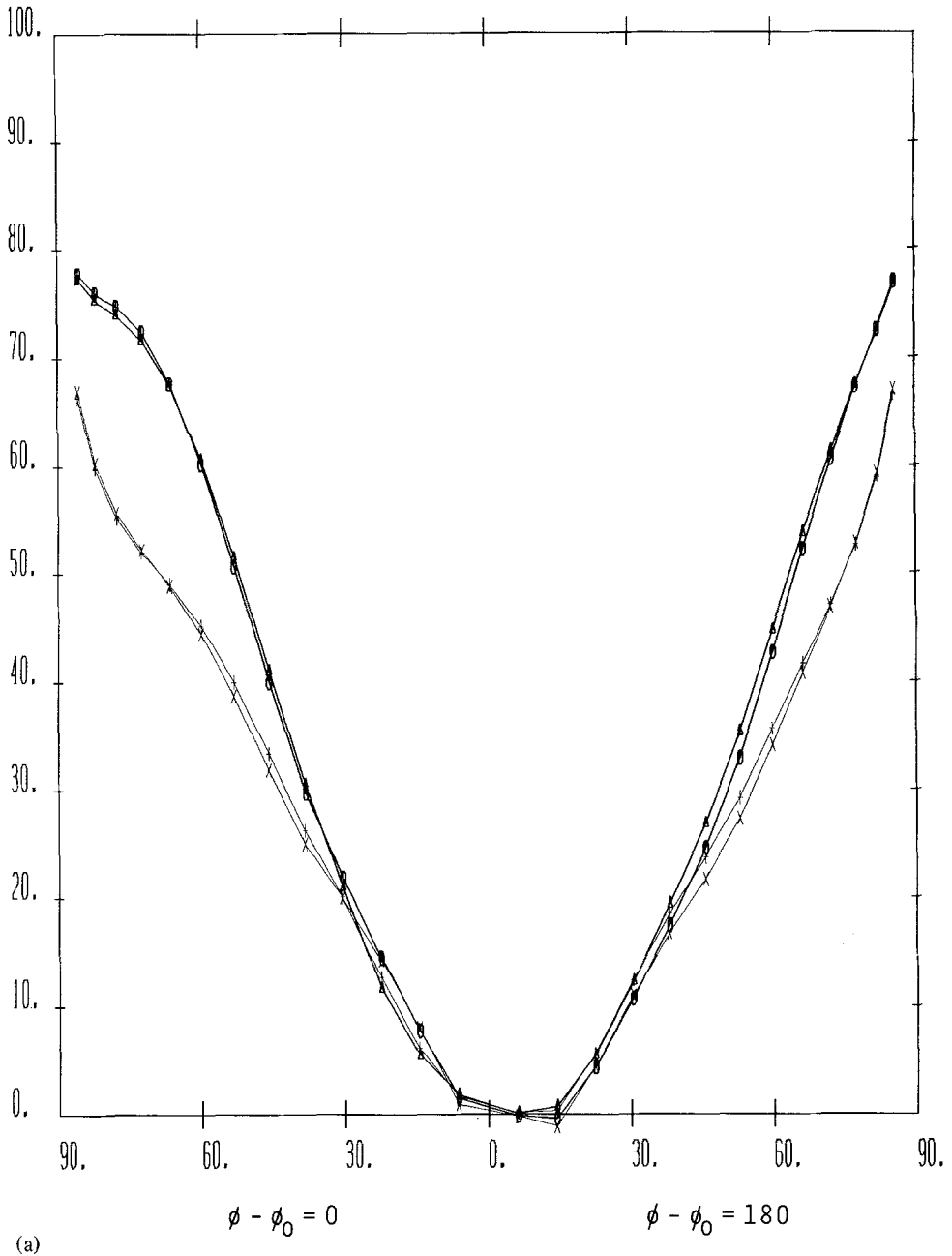
Fig. 5.   The same as Figure 4, but for degree of polarization.

Off the sun glint, the ocean surface does not show any appreciable effect. The polarization degree depends only upon the atmospheric condition. At $\theta_0 = 66.5°$ (Figure 5c), the polarization degree shows the saddle upward indicating two maxima. The one is located

(b)
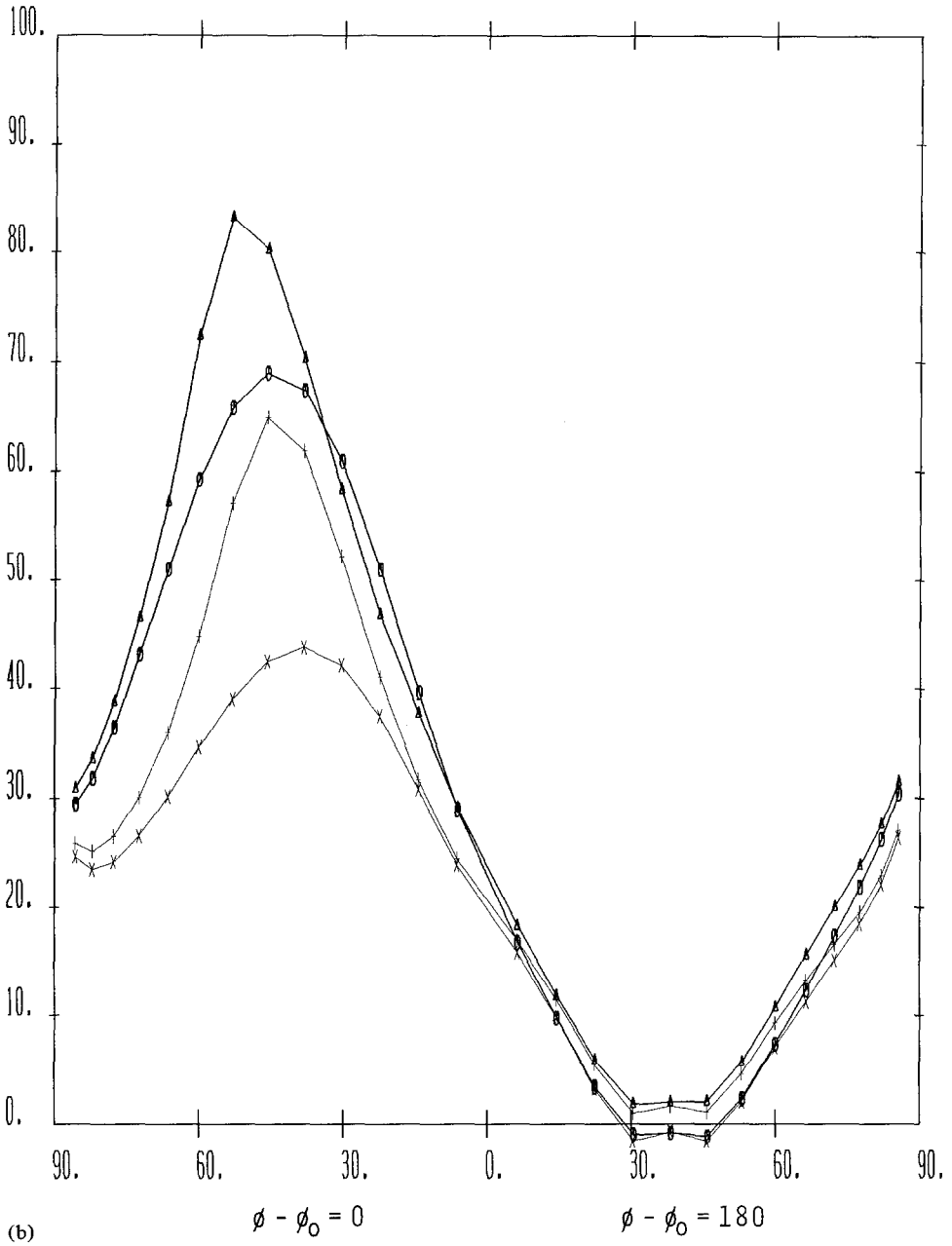
Fig. 5. *Continued.*

at around 80 deg away from the anti-solar direction due to the atmospheric scattering. The other is located at around the zenith angle of 55° due to the reflection process by the surface. Figure 6a shows the diffusely reflected radiation upwards from the atmosphere
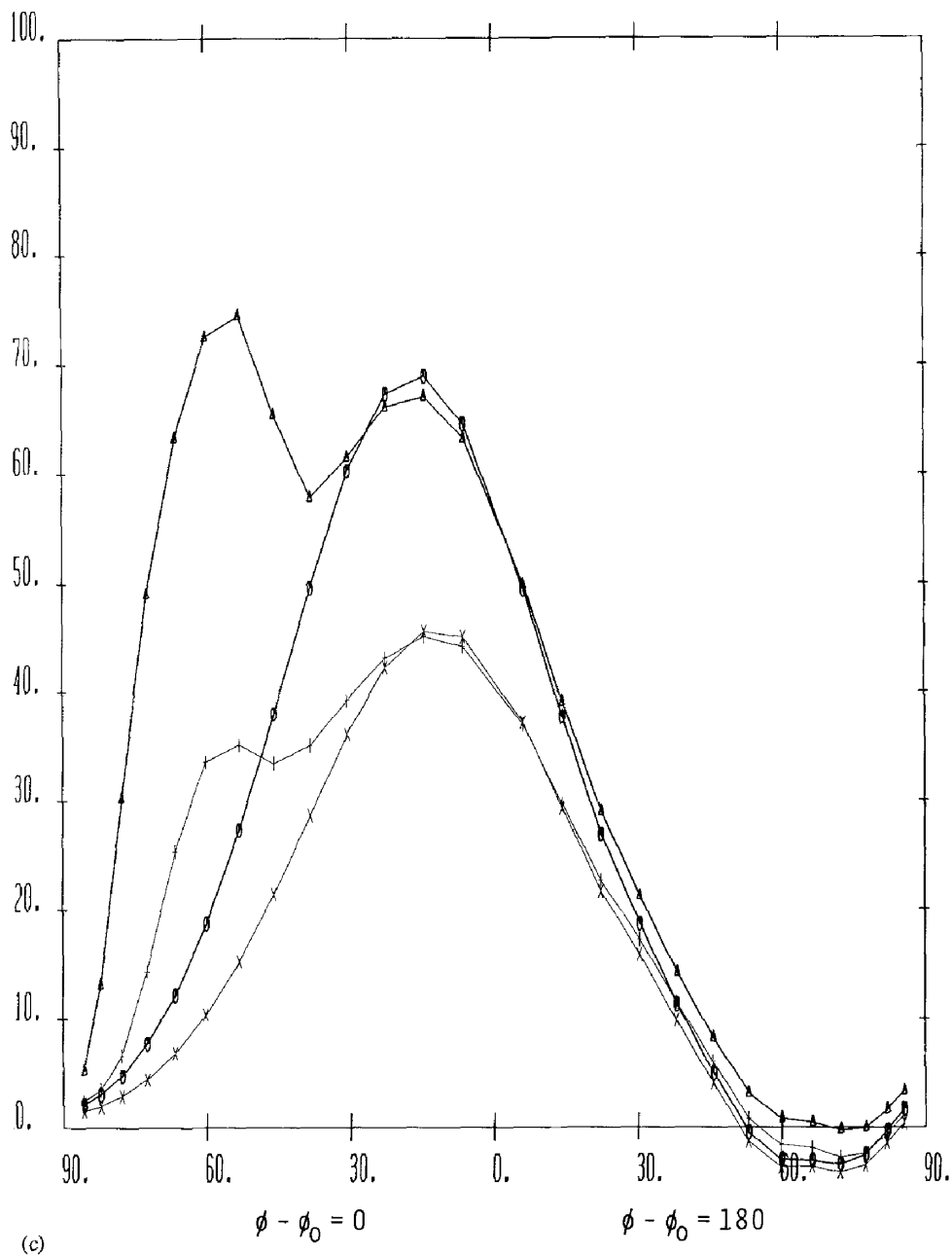
Fig. 5. *Continued.*

bounded by the ocean surface with the surface wind of 2 m s^{-1} and 8 m s^{-1} for $\theta_0 = 38.2°$. The symbols, ○ and △, denote the clear condition with wind of 2 m s^{-1} (c-2) and 8 m s^{-1} (c-8), respectively, whereas the symbols, × and + denote the hazy condition with wind
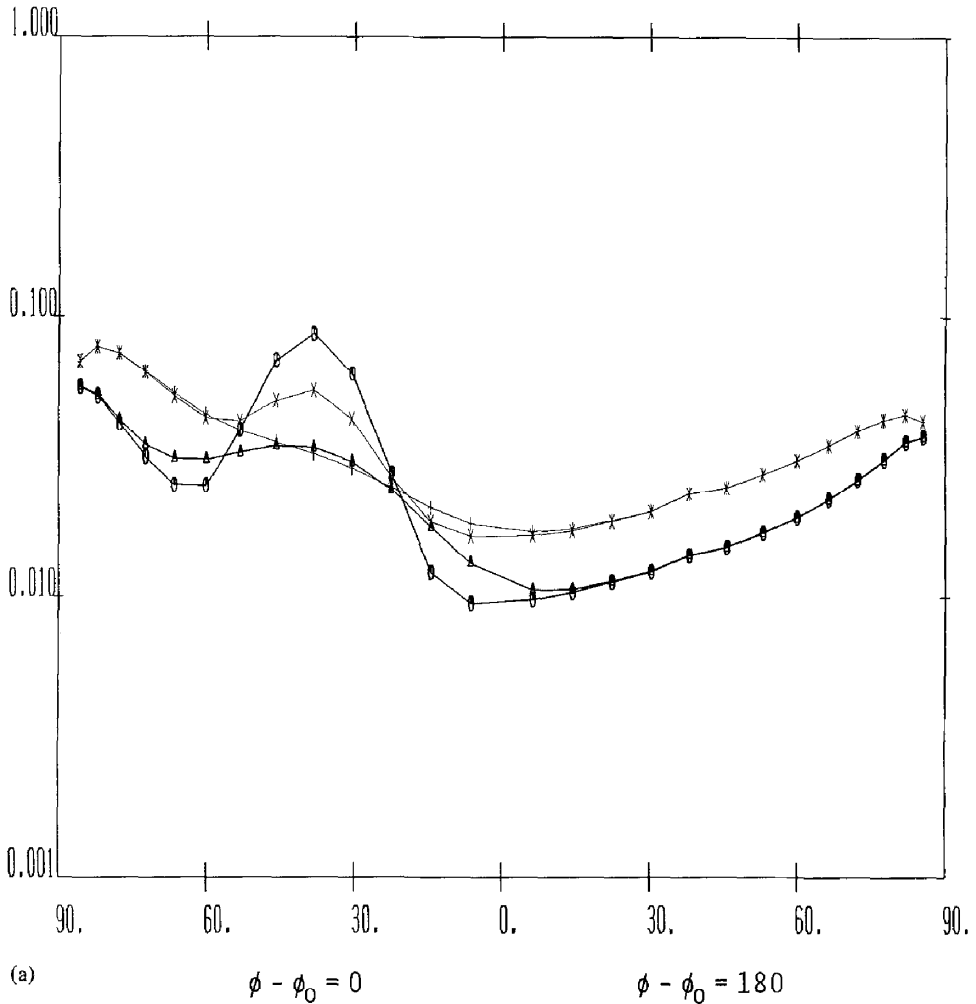
Fig. 6.   The effect of the surface wind upon the upwelling radiation from the atmosphere bounded by the ocean surface. $\theta_0 = 38.2°$. The symbols, o, △, ×, and + denote clear and 2 m s^{-1}, clear and 8 m s^{-1}, hazy and 2 m s^{-1}, and hazy and 8 m s^{-1}, respectively. (a) Intensity and (b) degree of polarization.

of 2 m s^{-1} (h-2) and 8 m s^{-1} (h-8), respectively. With the increase of the surface wind speed and with the increase of the atmospheric turbidity, the intensely reflected radiation in the sun glint decreases very much. The peak intensity in the sun glint is 0.087 for c-2 and decreases to 0.055 for h-2, whereas it decreases 0.052 from c-2 to c-8. There is no peak value for h-8. Off the sun glint the wind speed does not show any appreciable effect on the upwelling radiation. The corresponding peak value of the polarization degree in the sunglint for c-2 is 83% and decreases to 65% for h-2. It decreases 1.8% and 7.3% from c-2 to c-8 and from h-2 to h-8, respectively. Thus the effect of the atmosphere or that of the ocean surface on the radiative transfer can be simultaneously investigated in the observations of the intensity and the polarization degree of the upwelling radiation.

(b) $\phi - \phi_0 = 0$ $\phi - \phi_0 = 180$
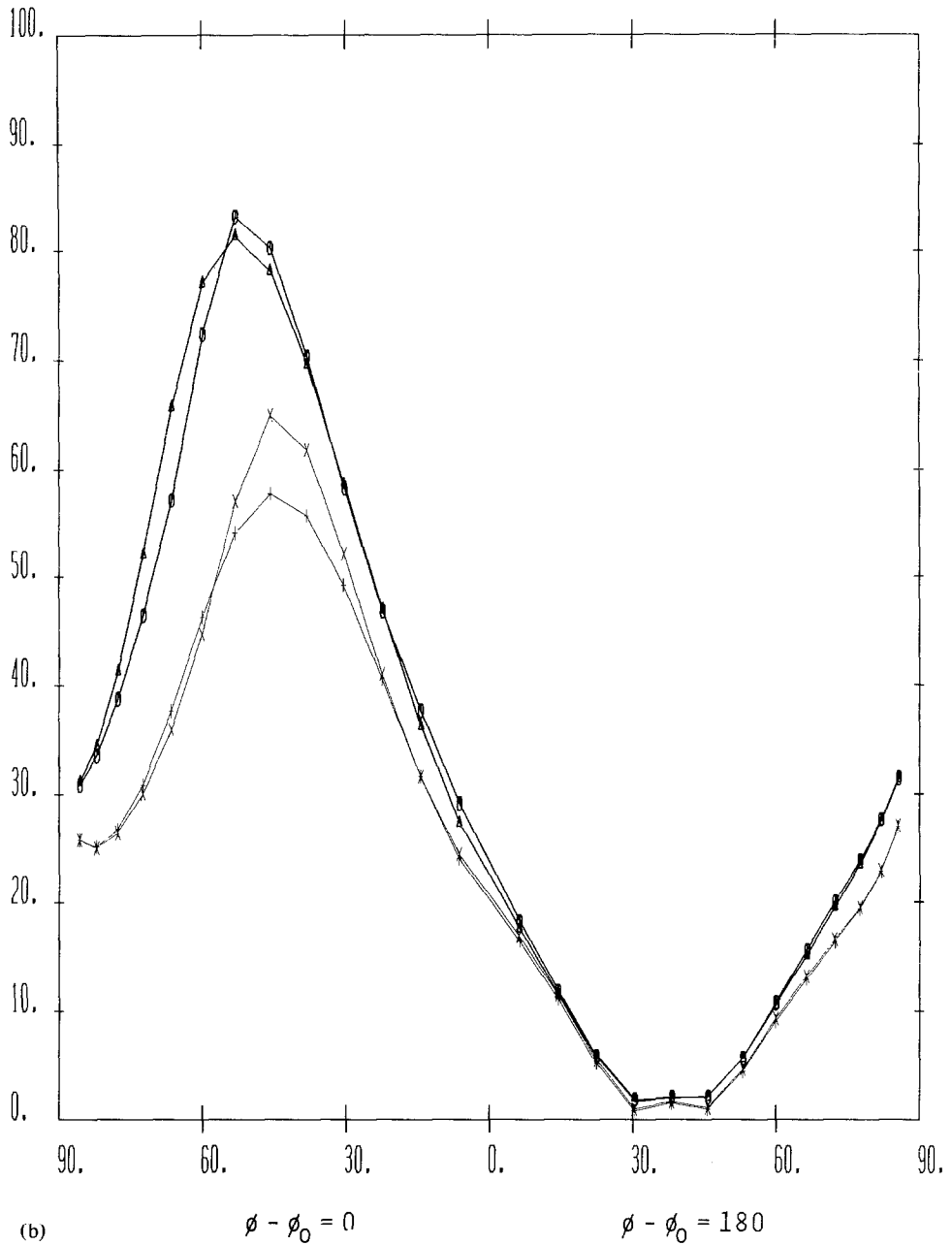
Fig. 6.   *Continued.*

Table IV shows the albedo (%) of the atmosphere ocean system as a function of the incident zenith angles (θ_0) at wavelength of $0.60\,\mu$m. The radiation transmitted from beneath the ocean surface is also taken into account, where the upwelling radiation is due

TABLE IV

The albedo (%) of the atmosphere-ocean system as a function of the solar zenith angles. The atmospheric condition is clear or hazy, whereas ocean water is under medium or turbid condition with the hydrosols of the refractive index of 1.16 or 1.07–*i*0.01.

Atm	Water	m	w	6.3	22.5	38.2	53.1	66.5	77.6	85.7
c	medium	1.16	2	5.75	5.96	6.83	8.97	13.51	21.65	29.06
			5	5.71	5.96	6.82	8.94	13.43	21.71	29.14
			8	5.66	5.94	6.80	8.90	13.38	21.74	29.18
		1.07	2	5.71	5.95	6.80	8.95	13.49	21.63	29.05
		−*i*0.01	5	5.66	5.93	6.79	8.91	13.41	21.69	29.13
			8	5.62	5.90	6.76	8.87	13.35	21.72	29.17
	turbid	1.16	2	6.19	6.13	7.11	9.25	13.75	21.81	29.15
			5	6.15	6.32	7.23	9.30	13.73	21.92	29.26
			8	6.10	6.35	7.21	9.27	13.68	21.96	29.31
		1.07	2	5.74	5.96	6.82	8.97	13.50	21.64	29.06
		−*i*0.01	5	5.69	5.95	6.81	8.93	13.43	21.70	29.13
			8	5.65	5.92	6.79	8.89	13.38	21.74	29.18
h	medium	1.16	2	8.26	8.88	10.73	14.75	22.17	32.06	33.82
			5	8.22	8.87	10.72	14.73	22.15	32.07	33.82
			8	8.18	8.84	10.70	14.70	22.13	32.08	33.82
		1.07	2	8.23	8.86	10.70	14.73	22.15	32.04	33.82
		−*i*0.01	5	8.19	8.84	10.69	14.70	22.12	32.06	33.81
			8	8.14	8.81	10.66	14.67	22.10	32.06	33.81
	turbid	1.16	2	8.62	9.06	10.98	14.98	22.36	32.19	33.90
			5	8.62	9.21	11.07	15.04	22.39	32.25	33.93
			8	8.58	9.23	11.06	15.02	22.38	32.26	33.93
		1.07	2	8.25	8.88	10.72	14.74	22.16	32.05	33.82
		−*i*0.01	5	8.21	8.86	10.71	14.72	22.14	32.07	33.82
			8	8.17	8.83	10.69	14.70	22.12	32.07	33.82

to the scattering by the ocean water and hydrosols. The albedo increases monotonically with the increase of the incident solar zenith angle. This is mainly due to the contribution of the scattered radiation in the atmosphere upon the flux. The albedo is 5.75, 8.97, and 29.06% for the solar zenith of 6.3°, 53.1°, and 85.7°, respectively for the clear atmosphere with the medium turbid ocean water ($m = 1.16$), where the isotropic surface wind is $2\,\mathrm{m\,s^{-1}}$. Whereas for a turbid ocean ($m = 1.16$), the albedo is 6.19% at $\theta_0 = 6.3°$ with the surface wind of $2\,\mathrm{m\,s^{-1}}$. It decreases once with the increase of the value of θ_0, and then increases monotonically with the increase of θ_0. It is 6.13% at $\theta_0 = 22.5°$, and is 7.11% at $\theta_0 = 38.2°$. This is partly due to the computational accuracy of the transmitted radiation from beneath the ocean surface. The albedo increases 0.5% at $\theta_0 = 6.3°$ due to the effect of the transmitted radiation from beneath the ocean surface. It is 0.19% at $\theta_0 = 22.5°$, and 0.33% at $\theta_0 = 38.2°$ (Table III). For a medium turbid ocean water, the same contribution upon the albedo is 0.07% at $\theta_0 = 6.3°$, 0.02% at $\theta_0 = 22.5°$, 0.05%
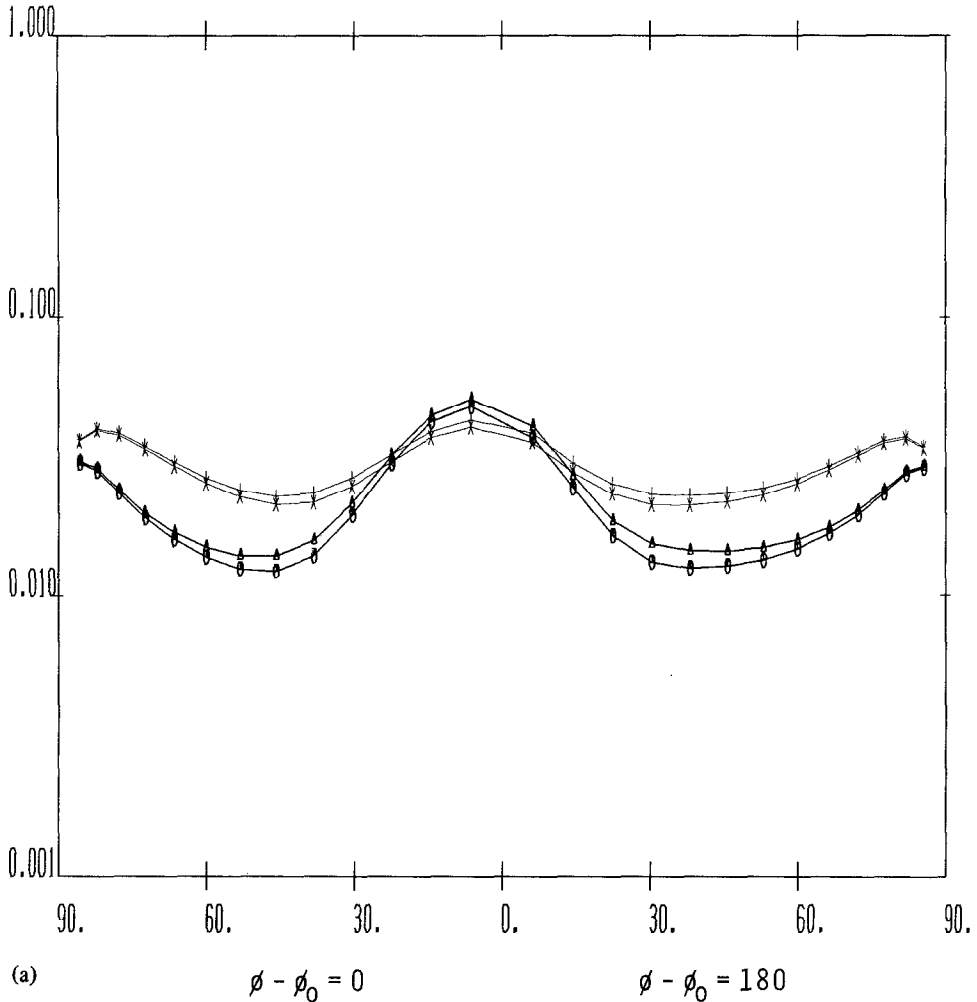
Fig. 7. The effect of the transmitted radiation from the turbid ocean ($m = 1.16$) on the upwelling radiation in the principal plane ($w = 5 \, \mathrm{m \, s^{-1}}$). Ordinate indicates intensities of the radiation. The symbols, o, △, ×, and + denote AS-c, AO-c, AS-h, and AS-h, respectively. (a) 6.3°, (b) 38.2°, and (c) 66.5°.

at $\theta_0 = 38.2°$. In the case of the refractive index of $1.07-i0.01$, the albedo increases monotonically with the increase of the solar zenith. This is mainly due to a little contribution of the transmitted radiation into the atmosphere. Thus in the wavelength of $0.60 \, \mu\mathrm{m}$, with the aid of the computational results of the two extreme model hydrosols, the contribution of the transmitted radiation from beneath the ocean surface into the atmosphere is at most 10% upon the flux of the upwelling radiation at the top of the atmosphere, whereas the atmospheric condition affects 45% upon the flux at $\theta_0 = 6.3°$. Therefore there is very little information to derive the optical characteristics and the density of the hydrosols. Figure 7a shows the intensity of the upwelling radiation from

(b) $\phi - \phi_0 = 0$ $\phi - \phi_0 = 180$
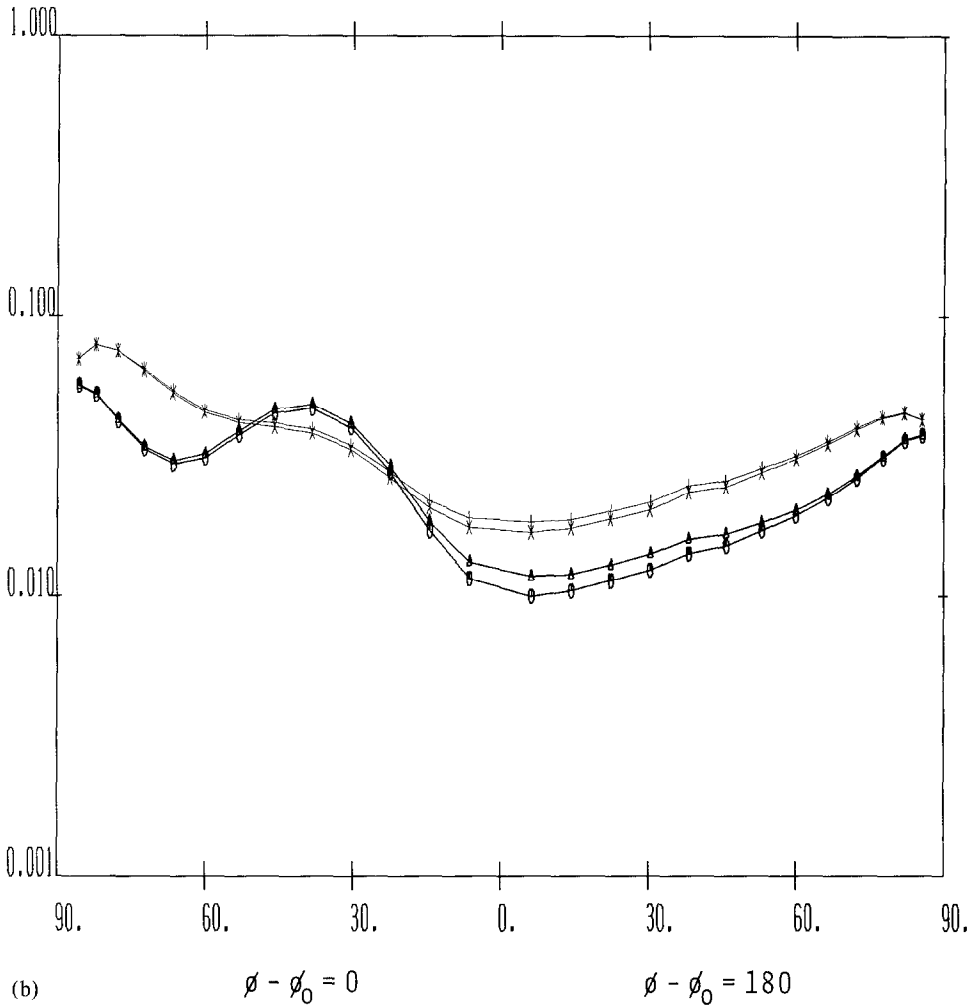
Fig. 7.   *Continued.*

the atmosphere ocean system at the solar zenith angle of $6.3°$ in the principal plane, where the incident solar flux is normalized to be 1. The symbols, $\circ$ and $\triangle$, denote the upwelling radiation from the clear atmosphere bounded by the ocean surface with wind of $5\,m\,s^{-1}$ (AS-c) and the corresponding radiation from the atmosphere-ocean system (AO-c), respectively, where the effect of the transmitted radiation from the turbid ocean into the atmosphere was taken into account (refractive index of hydrosols was assumed to be 1.16). The symbols, $\times$ and $+$, denotes the same as those of $\circ$ and $\triangle$, but for the hazy atmosphere. The radiance of the atmosphere ocean system is slightly larger than that of the atmosphere bounded by the ocean surface. At the zenith angle of observation $\theta = 30.4°$ on the solar side ($\phi - \phi_0 = 0$), the radiance increases 10.4% and 7.3% for clear and hazy conditions, respectively. Thus the effect of the transmitted radiation from the

$\phi - \phi_0 = 0$ $\phi - \phi_0 = 180$

(c)
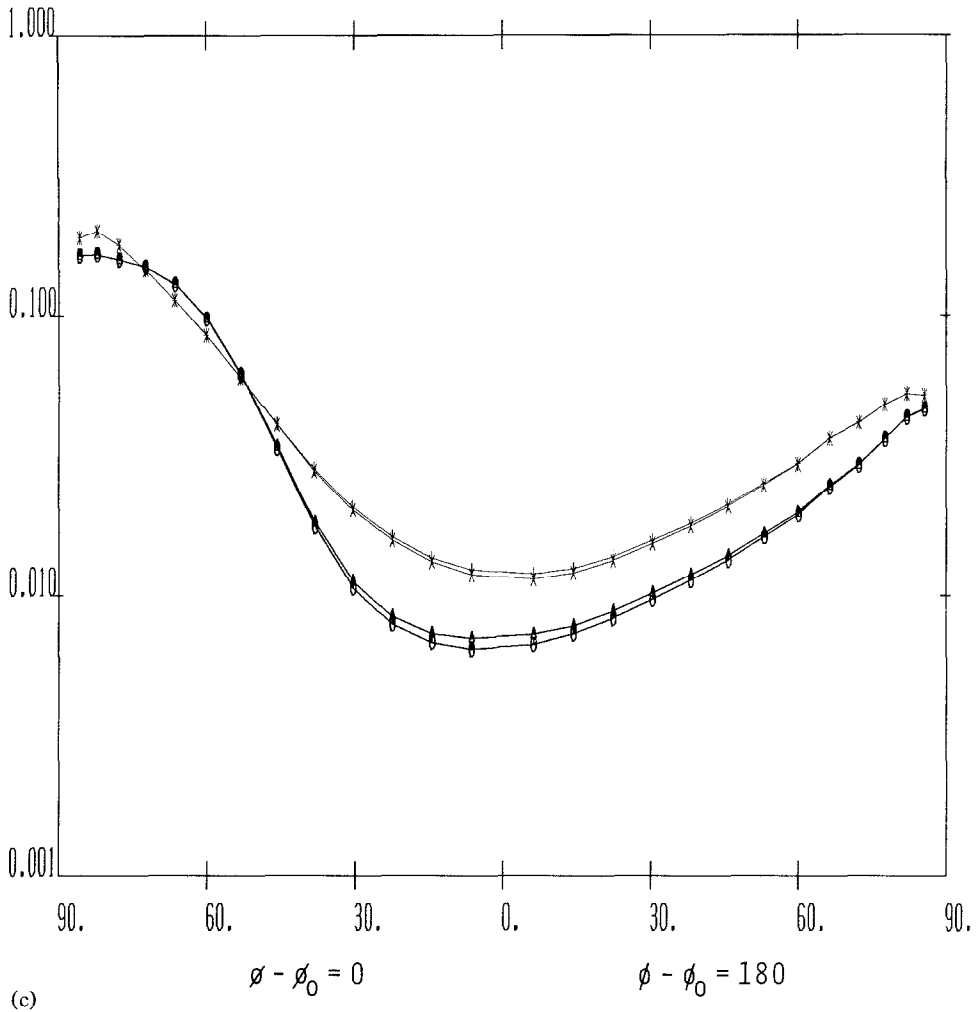
Fig. 7. *Continued.*

ocean into the atmosphere is not so large. First of all this is mainly due to the strong absorption of water at this wavelength region, in showing the fact that more than 99% of the incident radiation into the ocean is absorbed at the depth of 6 m. Secondary this is partly due to the scattering characteristics of hydrosols. A measure of the scattering in the lateral directions is expressed by the phase function asymmetry factor. As for the hydrosols with the refractive index of 1.16 and 1.07–i0.01, the asymmetry factor is 0.880 12 and 0.942 00, respectively, whereas the aerosols in the atmosphere ($m = 1.332$) is 0.753 63. Therefore the radiation is mainly scattered forwards by hydrosols. Hence the radiation scattered backward is very small. Furthermore this little amount of the radiation scattered backwards is mostly absorbed by water when it reaches the ocean-atmosphere boundary. Figure 7b shows the same as Figure 7a, but for $\theta_0 = 38.2°$. If the zenith angle

T. TAKASHIMA

(a) $\phi - \phi_0 = 0$ $\phi - \phi_0 = 180$
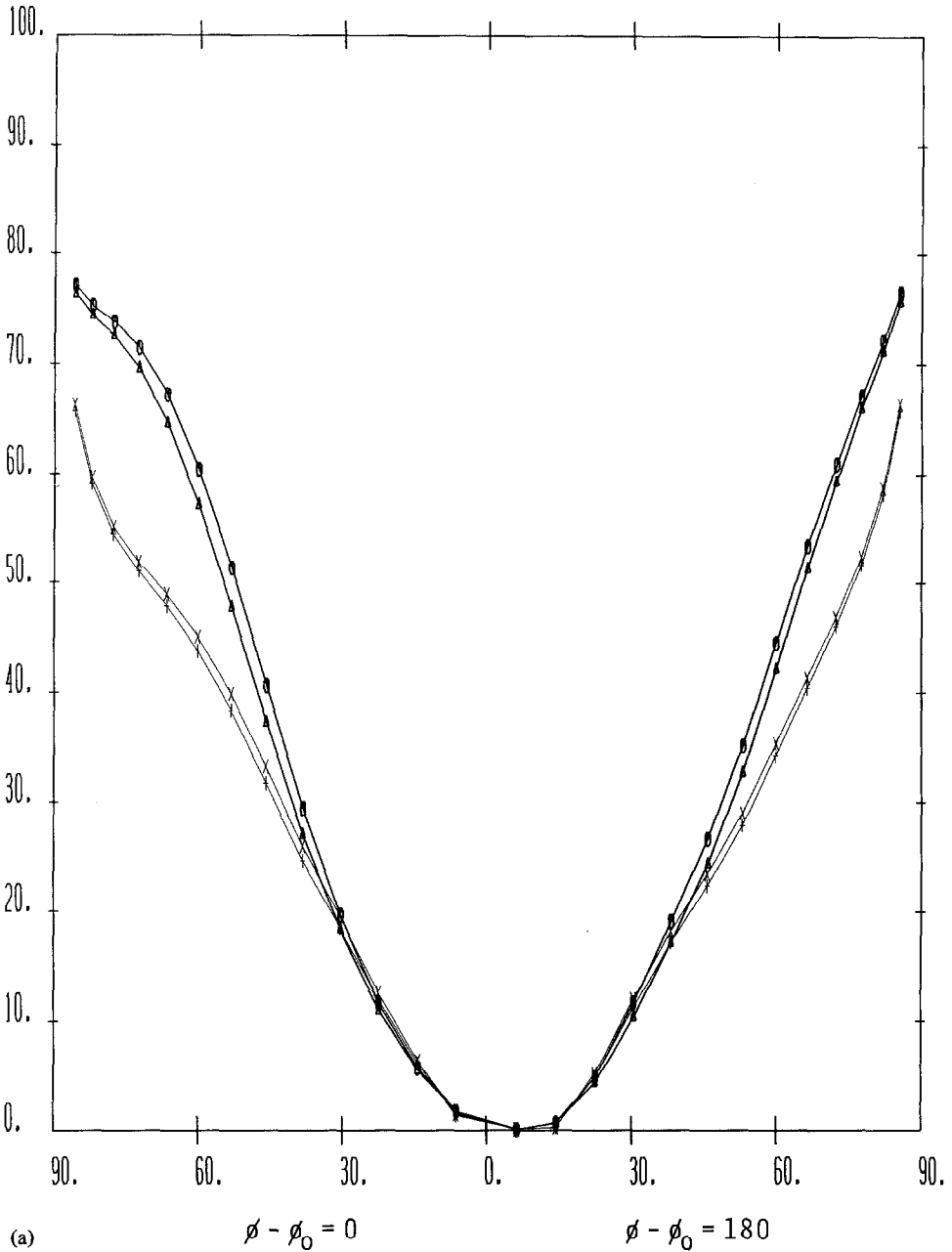
Fig. 8.   The same as Figure 7, but for the degree of polarization.

of observation is within 60°, the effect of the transmitted radiation from the ocean into the atmosphere is noted, but beyond 60°, there is no appreciable effect on the upwelling radiation. Figure 7c shows the same as Figure 7b, but for $\theta_0 = 66.5°$. If θ is over 40°,

(b) $\phi - \phi_0 = 0$ $\phi - \phi_0 = 180$
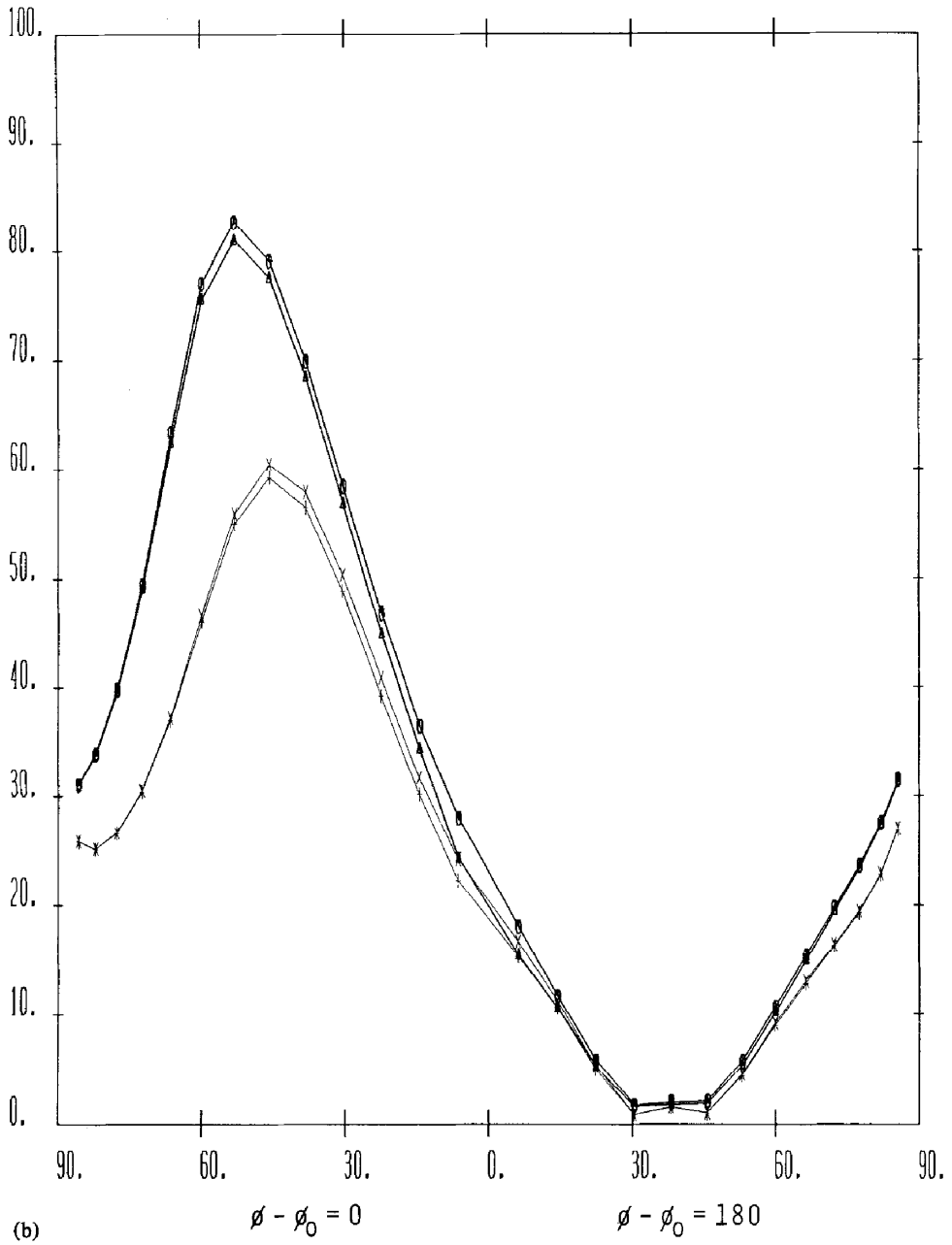
Fig. 8.   *Continued.*

there is no appreciable effect of the transmitted radiation on the upwelling radiation. Thus with the increase of the zenith angle of the incident solar flux, the effect of the transmitted radiation from the ocean into the atmosphere decreases.
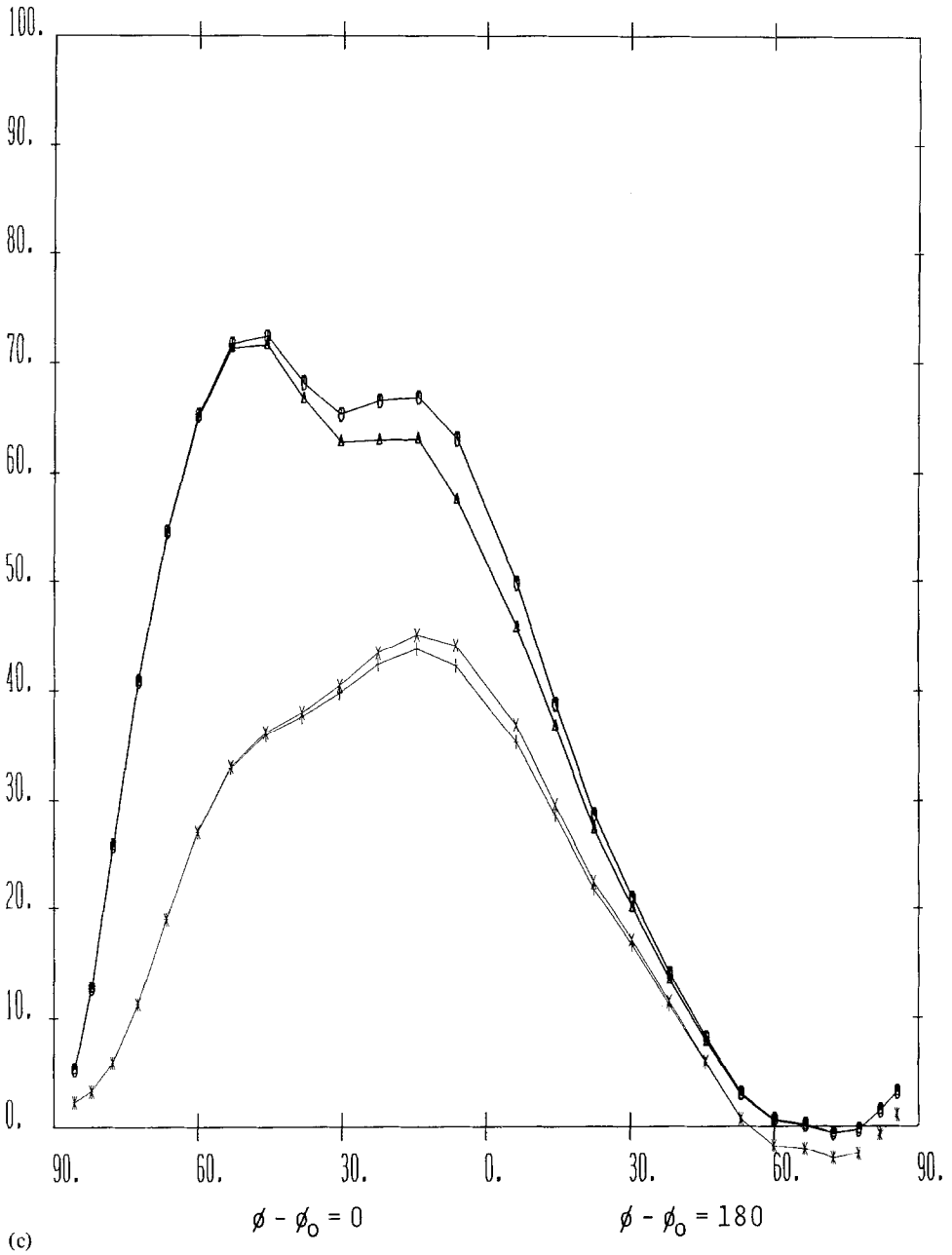
Fig. 8. *Continued.*

The corresponding degree of polarization is also shown in Figure 8a, b, and c. In Figure 8a, with the increase of the zenith angle, the degree of polarization increases monotonically in both cases of clear and hazy conditions. This is due to the fact that

the polarization degree increases when the direction is away from the incident direction, and it reaches the maximal value around 90 deg away from the incident direction. The polarization degree decreases slightly due to the effect of the radiation from the ocean. However the atmospheric condition affects the polarization degree much more than the radiation from the ocean. To study the effect of the hydrosols upon the upwelling radiation more precisely, the additional computations of the upwelling radiation should be undertaken in the wavelength region ranging from 0.40 to 0.50 μm, where the absorption effect of the ocean water is much less in comparison with that of 0.60 μm.

As for the accuracy of computations is concerned, the flux is a little overestimated on computing the radiation reflected by the ocean surface due to the computational system adopted at the present work. Here the shifted 15th Legendre polynomial was adopted in the computations of the atmospheric scattering, whereas that of 24th was adopted in the oceanic scattering. The error is rather independent of the incident solar zenith angles, whereas upon computing the radiation refracted by the surface, scattered diffusely by the hydrosols and water molecules, and then transmitted from the ocean water into the atmosphere, the error depends upon the incident solar zenith. The error is pronounced more with the lesser wind speed. At the wind speed of $2\,\mathrm{m\,s^{-1}}$ under a clear atmospheric condition with a turbid ocean model ($m = 1.16$), the error is estimated to be $+1.3\%$ at $\theta_0 = 6.3°$. The error becomes negative with the increase of the zenith angle. It is -3.2% at $\theta_0 = 22.4°$. However the error becomes very small when the angle is beyond $45°$, perhaps due to a small contribution of radiation travelling from the ocean into the atmosphere.

5. Conclusions

Polarization effect on radiative transfer in planetary atmosphere bounded by reflectors was previously discussed in detail by making use of the adding method (Takashima, 1984). The upwelling radiation at the top of the atmosphere-surface system can be calculated by using a single iterative equation in terms of the matrices of radiation diffusely reflected and transmitted by homogeneous sublayers in the atmosphere without requiring the equation for the diffuse transmission matrix of radiation (Takashima, 1973). Furthermore the upwelling radiance at the top and the downwelling radiance at the bottom of the atmosphere can be calculated by using only a couple of iterative equations in which the polarity effect of radiation is included (Takashima, 1975). The tiresome computations due to the polarity effect of radiation is overcome by these methods. At the present work, the adding method was extended to radiative transfer in the atmosphere-ocean system, where the air-water interface is separated by a ruffled surface, whose angular dependent reflection and refraction properties were calculated based on an isotropic Gaussian distribution of wave slopes (Cox and Munk, 1955). The atmosphere and the ocean are assumed to be horizontally homogeneous, whereas they are vertically inhomogeneous. It is not essential to adopt the assumption that the bottom of the ocean absorbs all incident radiation on it. In the diffuse radiation field, the ruffled ocean surface can be

thought of as an additional sublayer where the interaction of radiation is undertaken. The radiance incident on the ruffled ocean surface is partly refracted diffusely into the ocean water, is scattered diffusely upwards by the oceanic constituents, and is partly transmitted diffusely into the atmosphere and is partly reflected diffusely by the air-water boundary. Thus the ruffled ocean surface can be thought of as interacting interface. Therefore the upwelling radiation at the top of the atmosphere-ocean system can similarly be calculated by using a single iterative equation in which the polarity effect or radiation is included.

An example computation of the upwelling radiation at the top of the atmosphere was carried out at the wavelength of 0.60 micron, in which the effect of the ocean water absorption is strong. Computational results show the fact that due to the effect of the transmitted radiation from beneath the ocean, the polarization degree reduces a little in the directions where the effect of the atmospheric scattering is predominant, whereas it increases a little in the sun glint. The effect of the atmospheric scattering upon the polarization degree can be separated from that of the underlying ocean surface. To clarify these trend more precisely, the additional computations of the upwelling radiation should be undertaken in the wavelength region where the absorption effect of the ocean water is much less. Computational results of the upwelling radiance and the polarization degree of radiation in the region ranging from 0.40 micron to 0.75 micron are to be discussed separately.

Acknowledgement

References

Born, M. and Wolf, E.: 1964, *Principles of Optics*, Pergamon Press, Oxford.
Chandrasekhar, S.: 1950, *Radiative Transfer*, Clarendon Press, Oxford.
Cox, C. and Munk, W.: 1954a, *J. Mar. Res.* 13, 198.
Cox, C. and Munk, W.: 1954b, *J. Opt. Soc. America* 44, 838.
Cox, C. and Munk, W.: 1955, *J. Mar. Res.* 14, 63.
Hale, G. M. and Querry, M. R.: 1973, *App. Opt.* 12, 555.
Kneizys, F. X. *et al.*: 1980, Air Force Geophysics Lab., AFGL-TR-80-0067.
Morel, A.: 1974, *Optical Aspects of Oceanography* N. G. Jerlov and E. S. Nielsen (eds.), Chapt 1, Academic Press, London.
Nakajima, T. and Tanaka, M.: 1983, *J. Quant. Spectrosc. Radiat. Transfer* 29, 521.
Plass, G. N., Kattawar, G. W., and Guinn, J. A. Jr.: 1976, *Appl. Opt.* 15, 3161.
Raschke, E.: 1972, *Beit. Phys. Atmos.* 45, 1.
Sekera, Z.: 1966, Report for U.S. Air Force Project RAND, RM-4951-PR.
Selby, J. E. A. and McClatchey, R. M.: 1972, Air Force Cambridge Res. Lab. AFCRL-72-0745.
Takashima, T.: 1973, *J. Quant. Spectrosc. Radiat. Transfer* 13, 1229.

Takashima, T.: 1975, *Astrophys. Space Sci.* **36**, 319.

Takashima, T., Taggart, C. I. and Morrissey, E. G.: 1976, *Astrophys. Space Sci.* **40**, 157.

Takashima, T. and Takayama, Y.: 1981, *Pap. Met. Geophys.* **32**, 267.

Takashima, T.: 1983, *Pap. Met. Geophys.* **34**, 75.

Takashima, T.: 1985, *Appl. Math. Comp.*

Tanaka, M. and Nakajima, T.: 1977, *J. Quant. Spectrosc. Radiat. Transfer* **18**, 93.

Ueno, S.: 1960, *Astrophys. J.* **132**, 729.

Ueno, S.: 1981, *Proceedings 7th International Symp. Machine Process,* Remote Sensed Data, Purdue Univ., pp. 703–710.

Appendix A

Transformation of the slope components z_x and z_y into the directional solid angles in the meridian coordinates is described. These components are expressed by a function of the tilt β and the azimuth of the facet's ascent α. Let us consider the spherical triangle determined by the incident $\Omega'(\theta', \phi')$, emergent $\Omega(\theta, \phi)$ and normal $\Omega_0(\theta_0, \phi_0)$ directions with respect to the facet (Figure a-1). Then the following relations are obtained with the aid of the spherical trigonometry,

$$\cos^2 \omega = (1/2) [\cos \theta \cos \theta' + \sin \theta \sin \theta' \cos (\phi - \phi') + 1], \tag{a-1}$$

$$\sin \alpha' = \sin (\phi - \phi') \sin \theta / \sin 2\omega, \tag{a-2}$$

$$\cos \alpha' = [\sin \theta' \cos \theta - \cos \theta' \sin \theta \cos (\phi - \phi')] / \sin 2\omega, \tag{a-3}$$

$$\sin \omega / \sin (\phi_0 - \phi') = \sin \theta_0 / \sin \alpha', \tag{a-4}$$

$$\cos \omega = \cos \theta_0 \cos \theta' + \sin \theta_0 \sin \theta' \cos (\phi_0 - \phi'), \tag{a-5}$$

$$\sin \omega \cos \alpha' = \sin \theta' \cos \theta_0 - \cos \theta' \sin \theta_0 \cos (\phi_0 - \phi'), \tag{a-6}$$

Equations (a-5) and (a-6) yield

$$\cos \beta = \cos \theta' \cos \omega + \sin \omega \cos \alpha' \sin \theta', \tag{a-7}$$

where $\theta_0 = \beta$. With the aid of Equations (a-3) and (a-1), we have Equation (a-7) in the form

$$\cos \beta = (\cos \theta' + \cos \theta)/(2 \cos \omega). \tag{a-8}$$

With Equations (a-2), (a-4), and (a-8), we have the slope component z_x with respect to the incident and emergent directions according to

$$z_x = \sin \alpha \tan \beta$$
$$= \sin \theta |\sin (\phi - \phi')|/(\cos \theta' + \cos \theta), \tag{a-9}$$

where $\alpha = \phi_0 - \phi'$. Similarly Equation (a-5) can be transformed into the form

$$\cos \omega / \cos \beta = \cos \theta' + \sin \theta' z_y, \tag{a-10}$$

or

$$z_y = [\cos \omega / \cos \beta - \cos \theta'] / \sin \theta'. \tag{a-11}$$
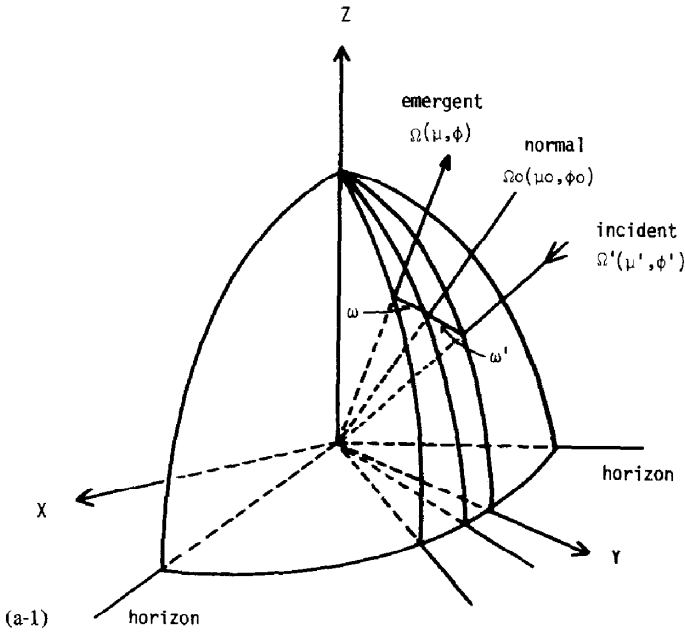
Fig. a-1.   Diagram showing transformation of slope components into the directional solid angles in the meridian coordinates. (a-2) Geometry of the facets expressed by the incident, emergent and normal directions.
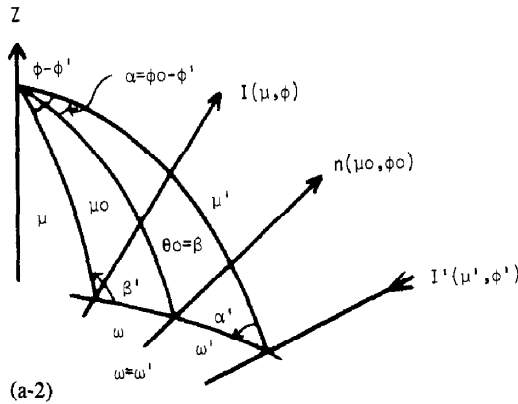
Fig. a-2.

Substitution of Equations (a-1) and (a-8) into (a-11) yields the slope component z_y as a function of the incident and emergent directions in the form,

$$z_y = [\sin \theta' + \sin \theta \cos (\phi - \phi')]/(\cos \theta' + \cos \theta). \qquad (a\text{-}12)$$

Therefore the slope parameters $\delta z_x \delta z_y$ can be converted to the emergent solid angle $d\Omega$ according to

$$\delta z_x \delta z_y = |J| \, d\theta \, d\phi, \tag{a-13}$$

where Jacobian J is expressed by

$$J = \begin{vmatrix} \dfrac{\partial z_x}{\partial \theta} & \dfrac{\partial z_x}{\partial \phi} \\[2mm] \dfrac{\partial z_y}{\partial \theta} & \dfrac{\partial z_y}{\partial \phi} \end{vmatrix} \tag{a-14}$$

or

$$J = -\sin \theta / (\cos \theta' + \cos \theta)^3 \times$$

$$\times [1 + \cos \theta \cos \theta' + \sin \theta \sin \theta' \cos (\phi - \phi')]. \tag{a-15}$$

Therefore

$$\delta z_x \delta z_y = a / (\cos \theta' + \cos \theta) \, d\Omega, \tag{a-16}$$

where the directional parameter a is defined by

$$a(\theta, \theta', \phi - \phi') = [1 + \cos \theta \cos \theta' + \sin \theta \sin \theta' \cos (\phi - \phi')] /$$

$$/ (\cos \theta + \cos \theta')^2, \tag{a-17}$$

where $a > 0$ at $0 < \theta, \theta' < \pi/2$.

Appendix B

To apply the adding method, the atmosphere and the ocean are divided into number of homogeneous sublayers. The scattering characteristics in each sublayers are, first of all, derived independent of other sublayers. Then interaction of radiation between two sublayers is considered. To evaluate the radiation from the ocean, let us consider the ocean surface and ocean separately from the atmosphere-ocean system. The diffuse or direct radiation $\overline{I}^{(1)}(-\Omega_0)$ is incident on the ocean surface (Figure b-1). Then the refracted radiation into the ocean $\overline{I}^{(2)}$ is expressed by Equation (43) as
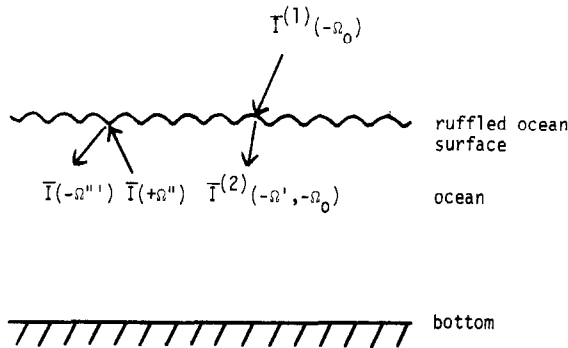
Fig. b-1.   Radiative transfer of the refracted radiation into the ocean.

$$\bar{I}^{(2)}(-\Omega', -\Omega_0) = (1/4\pi\mu')\,\bar{R}_T(-\Omega', -\Omega_0)\,\bar{I}^{(1)}(-\Omega_0). \tag{b-1}$$

Let us define the upward radiation and the downward radiation just beneath the ocean surface by $\bar{I}(+\Omega'')$ and $\bar{I}(-\Omega''')$, respectively. Then these radiations can be expressed with the Chandrasekhar's principle of invariance in the forms:

$$\mu''\bar{I}(+\Omega'') = (1/4\pi)\,\bar{S}_w(\tau_w, +\Omega'', -\Omega')\,\bar{I}^{(2)}(-\Omega') +$$
$$+ \{\bar{S}_w(\tau_w, +\Omega'', -\Omega''')\,\mu'''\bar{I}(-\Omega''')\}, \tag{b-2}$$

$$\mu'''\bar{I}(-\Omega''') = (1/4\pi)\,\bar{R}'_s(1/n, -\Omega''', +\Omega'')\,\bar{I}(+\Omega''), \tag{b-3}$$

where the hemispherical integration is defined by the brace { } (Sekera, 1960). These equations can easily be uncoupled by substituting Equation (b-3) into Equation (b-2) in the iterative form: i.e.,

$$\mu''\bar{I}(+\Omega'') = (1/4\pi)\,\bar{S}_w\,\bar{I}^{(2)}(-\Omega') + \{\bar{S}_w\{\bar{R}'_s(1/n)\mu''\bar{I}(+\Omega'')\}\} \tag{b-4}$$

where the directional parameters are abbreviated for simplicity. Therefore solution of Equation (b-4) can be written in infinite series of hemispherical integrations $\bar{R}'_s(1/n)$ $\bar{S}_w$ in the form

$$\mu''\bar{I}(+\Omega'') = \bar{S}_w\,[\bar{I} - \bar{R}'_s(1/n)\bar{S}_w]^{-1}\,\mu''\bar{I}^{(2)}(-\Omega''). \tag{b-5}$$

Thus it was shown that the intensity $\bar{I}(+\Omega'')$ equals that of $\bar{I}^{(3)}(+\Omega'')$ in Equation (49).

Appendix C

Upon calculating the matrix multiplications in Equations (38) and (42), let us consider the spherical triangle determined by the directions of the incident $\bar{I}(\Omega')$, reflection or refraction $\bar{I}(\Omega)$, and normal to the plain surface Z. The geometry of reflection or refraction is equivalent to that of transmission by scattering in the atmosphere. With the aid of a spherical trigonometry (see Figure a-1, 2), we have cosine of angles α' and β' appeared in rotation matrices in Equations (39) and (43) as

$$\cos\alpha' = \frac{\cos\theta - \cos 2\omega\cos\theta'}{\sin 2\omega\sin\theta'}, \tag{c-1}$$

$$\cos\beta' = \frac{\cos\theta' - \cos 2\omega\cos\theta}{\sin 2\omega\sin\theta}. \tag{c-2}$$

Similarly, we have sine of them as follows,

$$\sin\alpha' = \frac{\sin\theta\sin A}{\sin 2\omega}, \tag{c-3}$$

$$\sin\beta' = \frac{\sin\theta'\sin A}{\sin 2\omega}. \tag{c-4}$$

Therefore such parameters as $\cos 2\alpha'$, $\cos 2\beta'$, $\sin 2\alpha'$, and $\sin 2\beta'$ appeared in rotation matrices in Equations (39) and (43) can be written as

$$\cos 2\alpha' = 1 - 2\frac{(1-\mu^2)\sin^2 A}{1-\cos^2 2\omega}, \tag{c-5}$$

$$\cos 2\beta' = 1 - 2\frac{(1-\mu'^2)\sin^2 A}{1-\cos^2 2\omega}, \tag{c-6}$$

$$\sin 2\alpha' = 2\frac{\sin A}{1-\cos^2 2\omega}\sqrt{\frac{1-\mu^2}{1-\mu'^2}}\,[\mu - \mu'\cos 2\omega], \tag{c-7}$$

$$\sin 2\beta' = 2\frac{\sin A}{1-\cos^2 2\omega}\sqrt{\frac{1-\mu'^2}{1-\mu^2}}\,[\mu' - \mu\cos 2\omega]; \tag{c-8}$$

where

$$\cos 2\omega = \cos\theta'\cos\theta + \sin\theta'\sin\theta\cos A. \tag{c-9}$$

For the radiation reflected by the surface (see Equation (39)),

$$2\omega = 2\chi_i. \tag{c-10}$$

Similarly, for the radiation refracted by the surface (see Equation (43))

$$2\omega = \chi_i - \chi_t, \tag{c-11}$$

where the directional parameters μ'' and ϕ'' are placed for μ and ϕ, respectively. In the case of the reflected radiation by the surface, the probability of facets is expressed by the incident and reflected directions (see Equations (21) and (22)). In the case of the refracted radiation, in a manner similar to Appendix A, the probability of the facets is expressed by the incident and refracted directions. Let the directional parameter d be defined as

$$d = \cos\theta''\cos\theta' + \sin\theta''\sin\theta'\cos(\phi''-\phi'). \tag{c-12}$$

The orientation of the facets can be then expressed by the directions of the incident and the refracted radiations in the case of the radiation travelling from the atmosphere into the ocean according to

and
$$\cos\chi_t = (n-d)/(n^2-2nd+1)^{1/2} \quad \text{for} \quad 0 \leq \chi_t \leq \sin^{-1}(1/n) \tag{c-13}$$

$$\cos\chi_i = |nd-1|/(n^2-2nd+1)^{1/2}. \tag{c-14}$$

In the case of the radiation travelling from the ocean into the atmosphere,

and
$$\cos\chi_i = (1-nd)/(n^2-2nd+1)^{1/2} \quad \text{for} \quad 0 \leq \chi_i \leq \sin^{-1}(n) \tag{c-15}$$

$$\cos\chi_t = |n-d|/(n^2-2nd+1)^{1/2}. \tag{c-16}$$

It should be noted that the orientations of the facets can similarly be expressed by the directions of the incident and the reflected radiations according to

$$\cos \chi_i = [(d + 1)/2]^{1/2} \tag{c-17}$$

and

$$\cos \chi_t = [1 - (1 - d)/(2n^2)]^{1/2}. \tag{c-18}$$

Thus the slope components z_x and z_y can be expressed by the forms

$$z_x = \frac{\sin \chi_i \sin \alpha'}{\cos \theta' \cos \chi_i + \sin \theta' \sin \chi_i \cos \alpha'}, \tag{c-19}$$

$$z_y = \frac{\sin \theta' \cos \chi_i - \cos \theta' \sin \chi_i \cos \alpha'}{\cos \theta' \cos \chi_i + \sin \theta' \sin \chi_i \cos \alpha'}, \tag{c-20}$$

where parameters χ_i and χ_t are defined by the angles from the directions of the incident and refracted radiation to the normal direction to the orientation of a facet, respectively, where cosine and sine of the rotation angles α' are expressed in the forms,

$$\sin \alpha' = \frac{\sin (\phi'' - \phi')}{\sin (\chi_i - \chi_t)} \sin \theta'', \tag{c-21}$$

$$\cos \alpha' = \frac{\cos \theta'' - \cos \theta' \cos (\chi_i - \chi_t)}{\sin \theta' \sin (\chi_i - \chi_t)}. \tag{c-22}$$

Therefore the slope components are as follows:

$$z_x = \frac{\sin \theta'' \sin (\phi'' - \phi')}{\cos \theta'' - (1/n) \cos \theta'} \quad \text{at} \quad n \neq 1, \tag{c-23}$$

where $\phi'' - \phi' > 0$ at $n > 1$ and $\phi'' - \phi' < 0$ at $n < 1$, and

$$z_y = \frac{-(1/n) \sin \theta' + \sin \theta'' \cos (\phi'' - \phi')}{\cos \theta'' - (1/n) \cos \theta'} \quad \text{at } n \neq 1, \tag{c-24}$$

Therefore a parameter $z_x^2 + z_y^2$ appeared in the isotropic Gaussian distribution function $P(z_x^2 + z_y^2)$ can be written in the form

$$z_x^2 + z_y^2 = 2b(\theta'', \theta', \phi'' - \phi', n) - 1 - \frac{1 - (1/n)^2}{(\cos \theta'' - (1/n) \cos \theta')^2}, \tag{c-25}$$

where the directional parameter, b, is expressed in a manner similar to the parameter, a, in the case of the reflected radiation according to the form:

$$b(\theta'', \theta', \phi'' - \phi', n) =$$

$$= \frac{1 - (1/n) \cos \theta'' \cos \theta' - (1/n) \sin \theta'' \sin \theta' \cos (\phi'' - \phi')}{c (\theta'', \theta', n)}, \tag{c-26}$$

where the directional parameter, c, is expressed by the form,

$$c (\theta'', \theta', n) = \cos \theta'' - (1/n) \cos \theta'. \tag{c-27}$$

The slope parameter $\delta z_x \delta z_y$ can also be converted into a function of the solid angle $d\Omega''$ of the refracted radiation according to the form

$$\delta z_x \delta z_y = \left| \frac{b(\Omega'', \Omega', n)}{c(\theta'', \theta', n)} \right| d\Omega''. \tag{c-28}$$

The projected area normal to the incoming rays dS just above the ocean surface is expressed by the form

$$dS = \cos(\chi_i) \sec \beta P(z_x, z_y) \delta z_x \delta z_y. \tag{28}$$

The incident radiation on the facet is, therefore, given by

$$dS \, \bar{I}^{(1)}(-\Omega'). \tag{c-29}$$

The refracted radiation by the slope to the refracted direction χ_t downwards is

$$\bar{T}_{sp}(\chi_t, \chi_i) \, dS \, \bar{I}^{(1)}(-\Omega'). \tag{c-30}$$

Therefore, the refracted radiation by the ocean surface can be written as

$$\bar{I}(-\Omega'') \, d\Omega'' = \bar{T}_{sp}(\chi_t, \chi_i) \, dS \, \bar{I}^{(1)}(-\Omega'); \tag{c-31}$$

or the refraction matrix of the ocean surface, which corresponds to the reflection matrix $\bar{R}_s$ in Equation (33), can be introduced by the form

$$\bar{I}(-\Omega'') = (1/4\pi\mu'') \, \bar{R}_T(\chi_t, \chi_i) \, \bar{I}^{(1)}(-\Omega'). \tag{c-32}$$

Therefore, the diffuse refraction matrix of the ocean surface $\bar{R}_T(-\Omega'', -\Omega', n, w)$ can be written in the form given by Equation (43).